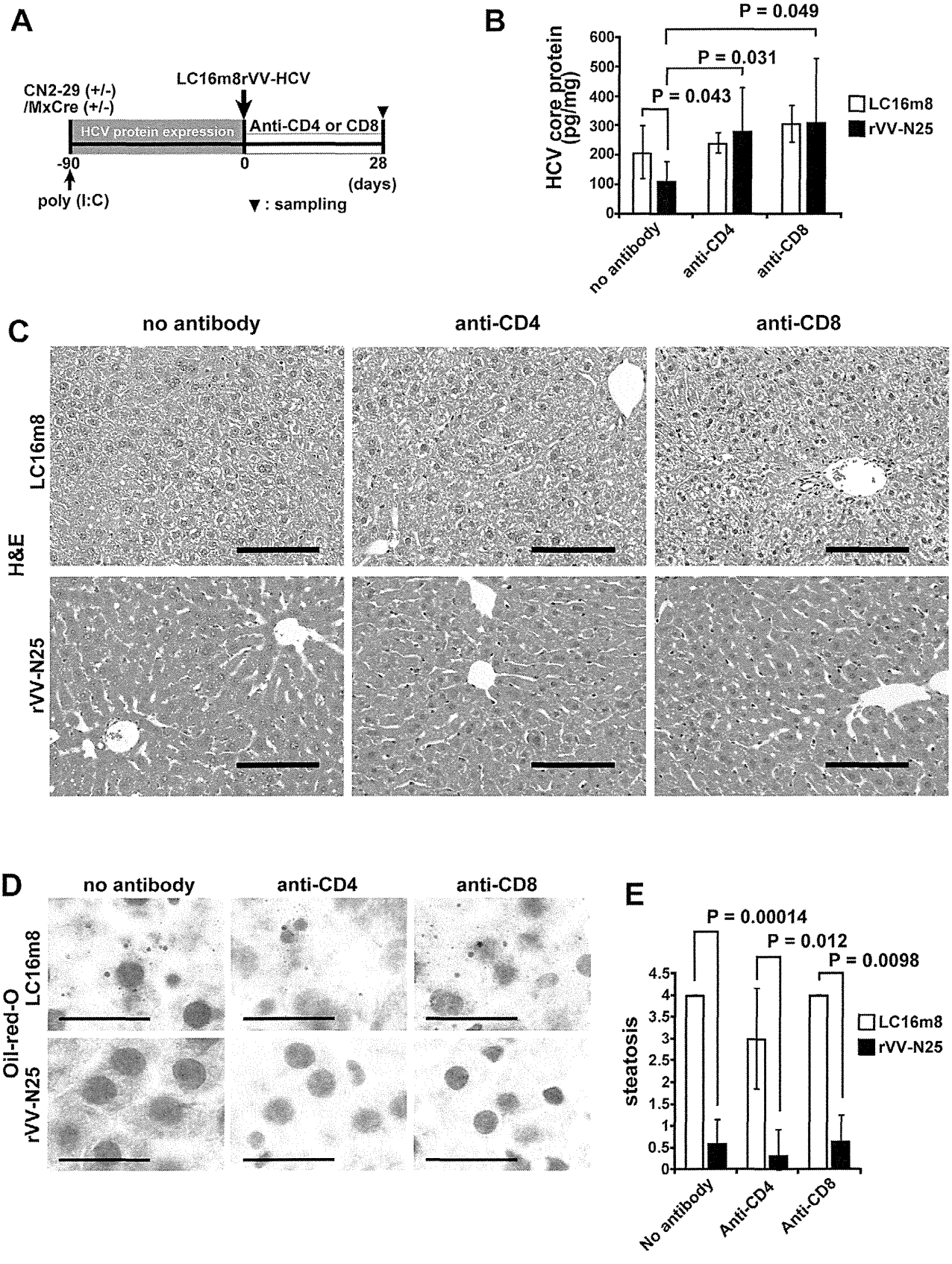

Figure 4. Role of CD4 and CD8 T cells in rVV-N25-treated mice. (**A**) Schematic diagram depicts depletion of CD4 and CD8 T cells via treatment with monoclonal antibodies. (**B**) Comparison of HCV core protein expression in control, CD4-depleted, and CD8-depleted mice 28 days after immunization with LC16m8 or rVV-N25. (**C, D**) Histological analysis of liver samples from CD4-depleted or CD8-depleted CN2-29$^{(+/-)}$/MxCre$^{(+/-)}$ mice

28 days after immunization with LC16m8 or rVV-N25. The scale bars indicate 100 μm (**C**) and 50 μm (**D**). (**E**) Histological evaluation of steatosis in liver samples from CD4-depleted or CD8-depleted CN2-29$^{(+/-)}$/MxCre$^{(+/-)}$ mice 28 days after immunization with LC16m8 or rVV-N25. Significant relationships are indicated by a P-value.
doi:10.1371/journal.pone.0051656.g004

a HCV nonstructural protein. Thus, we focused on the role of the NS2 region as the target for CD8 T cells and generated EL-4 cell lines that expressed the NS2 antigen or the CN2 antigen.

Isolated splenocytes from immunized mice were co-cultured with EL-4CN2 or EL-4NS2 cell lines for 2 weeks and analyzed.

Cytolytic cell activation can be measured using CD107a, a marker of degranulation [15]. The ratio of CD8$^+$CD107a$^+$ cells to all CD8 T cells significantly increased in rVV-N25-treated splenocytes after co-culture with EL-4CN2 or EL-4NS2 ($P<0.05$), whereas splenocytes that had been treated with any other rVV were not detected (Figure 5A, B and C). These results indicated that rVV-N25 treatment increased the frequency of HCV NS2-specific activated CD8 T cells. Consistent with these results, the ratio of CD8$^+$IFN-γ$^+$ cells to all CD8 T cells for rVV-N25-treated mice was also significantly higher than that for mice treated with any other rVV ($P<0.05$). Taken together, these findings indicated that rVV-N25 induced an effective CD8 T-cell immune response and that NS2 is an important epitope for CD8 T cells.

rVV-N25 Immunization Suppressed Inflammatory Cytokines Production

To determine whether rVV-N25 treatment affected inflammatory cytokine production, we measured serum levels of inflammatory cytokines after rVV immunization. The serum levels of these inflammatory cytokines increased in the CN2-29$^{(+/-)}$/MxCre$^{(+/-)}$ mice (Figure 6A, Figure S5). Immunization with rVV-N25 affected serum levels of inflammatory cytokines in CN2-29$^{(+/-)}$/MxCre$^{(+/-)}$ mice and caused a return to the cytokine levels observed in wild-type untreated mice (Figure 6A). In wild-type mice, the cytokine levels remained unchanged after immunization (Figure 6A). These results indicated that inflammatory cytokines were responsible for liver pathogenesis in the transgenic mice.

To test the hypothesis that inflammatory cytokines were responsible for liver pathogenesis in CN2-29$^{(+/-)}$/MxCre$^{(+/-)}$ mice, we administered transgenic mouse serum intravenously into nontransgenic mice. We observed the development of chronic hepatitis in the nontransgenic mice within 7 days after the serum transfer (Figures 6B and C). This finding was consistent with the

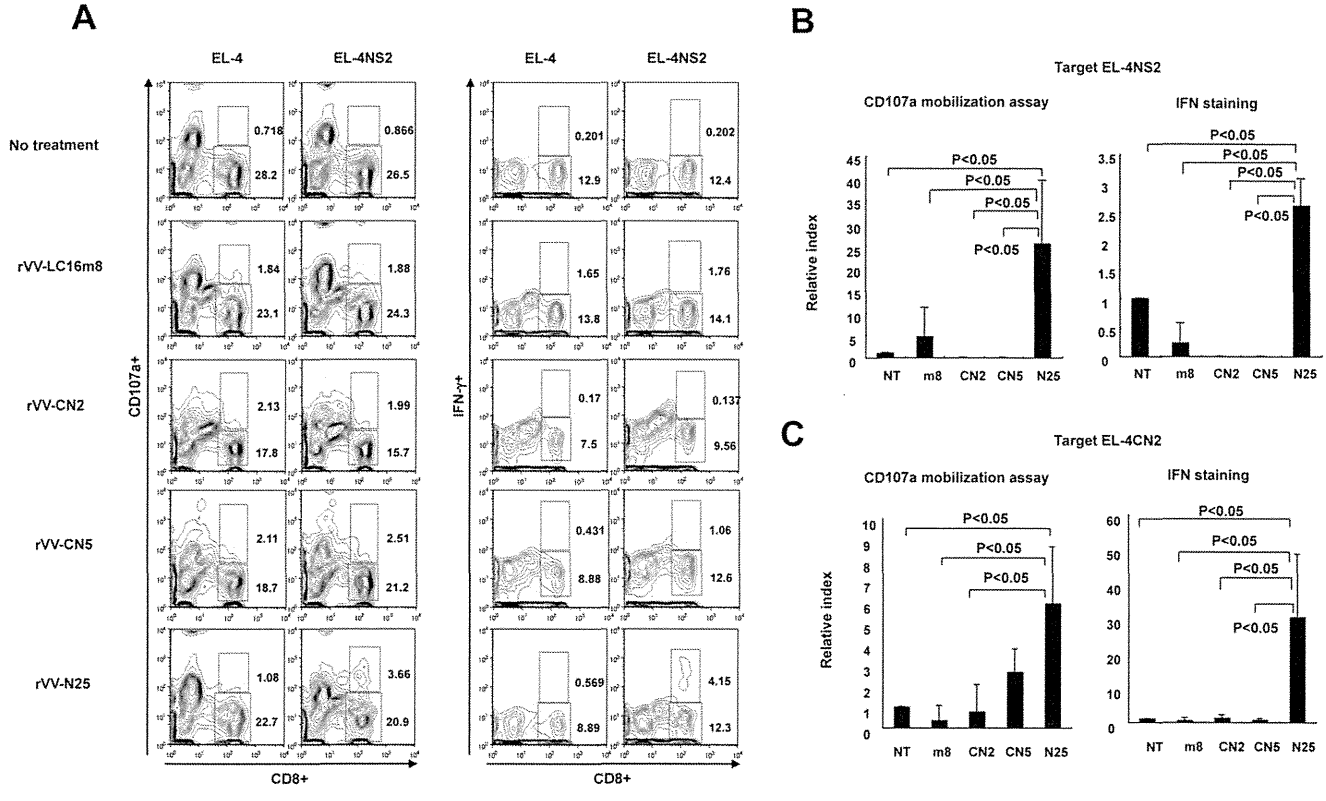

Figure 5. Immunization with rVV-N25 induced CD8 T-cell degranulation, a marker for cytotoxicity, and IFN-γ production. (**A**) The numbers represent the percentage of CD107a positive cells and negative cells (left two columns) and IFN-γ-positive cells and negative cells (right two columns). (**B, C**) The ratio of CD8$^+$IFN-γ$^+$ cells to all CD8 T cells for rVV-N25-treated mice was significantly higher than that for mice treated with any other rVV. Splenocytes (4×10^6 per well) were cultured with EL-4CN2 or EL-4NS2 cell lines in RPMI 1640 complete medium including 3% T-STIM^{TM} with ConA for 2 weeks. Harvested cells were incubated for 4 h with EL-4, EL-4CN2, or EL-4NS2 in combination with PE-labeled anti-CD107a mAb and monensin in RPMI 1640 complete medium with 50 IU/mL IL-2, according to the manufacturer's instruction. After incubation, cell suspensions were washed with PBS, and the cells were further stained with APC-labeled anti-IFN-γ mAb and Pacific blue-labeled anti-CD8 mAb. Harvested cells were stained with anti-CD107a-PE, anti-IFN-γ-APC, or anti-CD8-Pacific blue. Results that are representative of three independent experiments are shown. Significant relationships are indicated by P-value.
doi:10.1371/journal.pone.0051656.g005

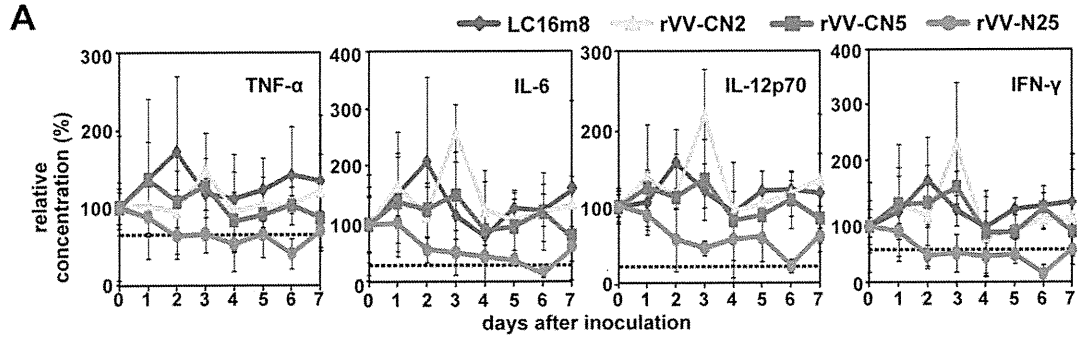
A
LC16m8
rVV-CN2
rVV-CN5
rVV-N25
TNF-α
IL-6
IL-12p70
IFN-γ
relative concentration (%)
days after inoculation

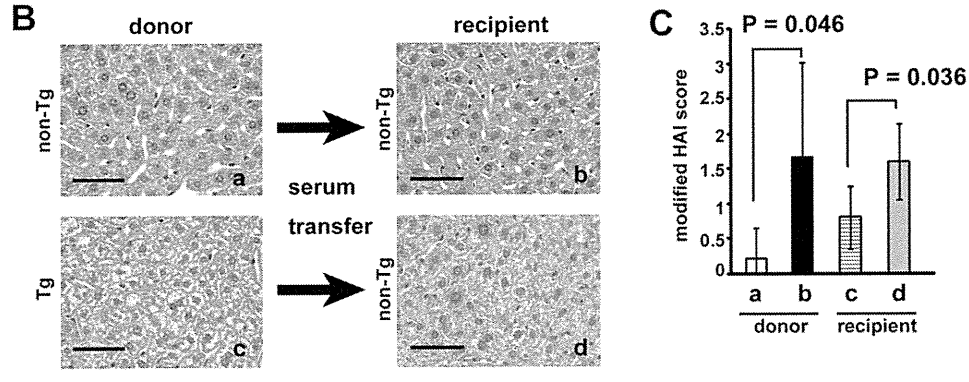
B
donor
recipient
non-Tg
Tg
serum transfer
a
b
c
d
C
P = 0.046
P = 0.036
modified HAI score
donor
recipient

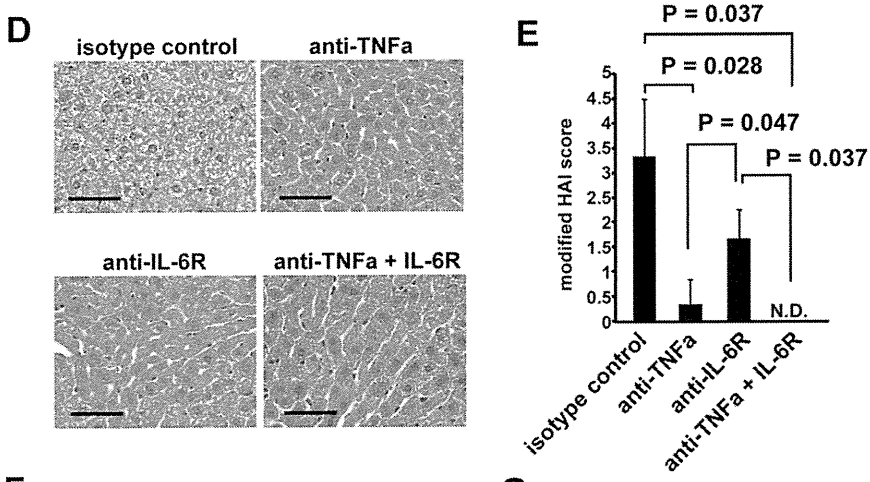
D
isotype control
anti-TNFa
anti-IL-6R
anti-TNFa + IL-6R
E
P = 0.037
P = 0.028
P = 0.047
P = 0.037
N.D.
modified HAI score
isotype control
anti-TNFa
anti-IL-6R
anti-TNFa + IL-6R

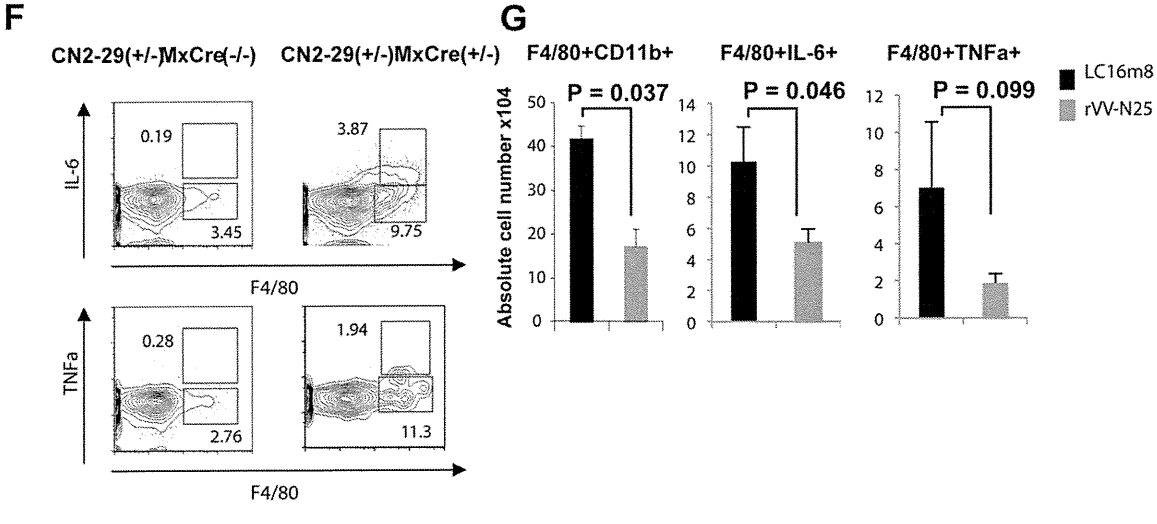
F
CN2-29(+/-)MxCre(-/-)
CN2-29(+/-)MxCre(+/-)
IL-6
TNFa
F4/80
0.19
3.45
3.87
9.75
0.28
2.76
1.94
11.3
G
F4/80+CD11b+
F4/80+IL-6+
F4/80+TNFa+
P = 0.037
P = 0.046
P = 0.099
Absolute cell number x10^4
LC16m8
rVV-N25

Figure 6. Immunization with rVV-N25 suppresses serum inflammatory cytokine levels. (**A**) Daily cytokine levels in the serum of CN2-29$^{(+/-)}$/MxCre$^{(+/-)}$ mice during the week following immunization with LC16m8, rVV-CN2, rVV-N25, or rVV-CN5. Values represent means ± SD (n = 3) and reflect the concentrations relative to those measured on day 0. The broken lines indicate the baseline data from wild-type mice. In all cases, n = 6 mice per group. (**B**) Liver sections from CN2-29$^{(+/-)}$/MxCre$^{(+/-)}$ and CN2-29$^{(+/-)}$/MxCre$^{(-/-)}$ mice. (**C**) Histology activity index (HAI) scores of liver samples taken from CN2-29$^{(+/-)}$/MxCre$^{(+/-)}$, or CN2-29$^{(+/-)}$/MxCre$^{(-/-)}$ mice. (**D**) Liver sections from CN2-29$^{(+/-)}$/MxCre$^{(+/-)}$ mice in which TNF-α was neutralized and the IL-6 receptor was blocked. The scale bars indicate 50 μm. (**E**) HAI scores of liver samples taken from CN2-29$^{(+/-)}$/MxCre$^{(+/-)}$ in which TNF-α was neutralized and the IL-6 receptor was blocked. Tg and non-Tg indicate CN2-29$^{(+/-)}$/MxCre$^{(+/-)}$ and CN2-29$^{(+/-)}$/MxCre$^{(-/-)}$, respectively. (F) Macrophages were the main producers of TNF-α and IL-6 in CN2-29$^{(+/-)}$/MxCre$^{(+/-)}$ mice following poly(I:C) injection. (G) Immunization with rVV-N25 reduced the number of macrophages in liver samples from CN2-29$^{(+/-)}$/MxCre$^{(+/-)}$ mice and suppressed TNF-α and IL-6 production from macrophages (Figure 6G). Significant relationships are indicated by a P-value.
doi:10.1371/journal.pone.0051656.g006

hypothesis that inflammatory mediators played a key role in inducing hepatitis. Furthermore, to investigate whether TNF-α and IL-6 played particularly critical roles in the pathogenesis of chronic hepatitis in the transgenic mice, we neutralized TNF-α and blocked the IL-6 receptor in the livers of these mice. As expected, chronic hepatitis did not develop in these mice. (Figure 6D and E).

Next, to determine which cell population(s) produced TNF-α, IL-6, or both during continuous HCV expression in CN2-29$^{(+/-)}$/MxCre$^{(+/-)}$ mice, we isolated intrahepatic lymphocytes (IHLs) and labeled the macrophages (the F4/80^{+} cells) with anti-TNF-α and anti-IL-6 antibodies using an intracellular cytokine detection method. Macrophages in CN2-29$^{(+/-)}$/MxCre$^{(-/-)}$ mice produced small amounts of TNF-α and IL-6, while those in CN2-29$^{(+/-)}$/MxCre$^{(+/-)}$ mice produced much larger amounts of these cytokines (Figure 6F).

Finally, we evaluated whether rVV-N25 treatment affected the number of macrophages, cytokine production by macrophages, or both; specifically, we isolated IHLs from CN2-29$^{(+/-)}$/MxCre$^{(+/-)}$ mice 7 days after immunization with rVV-N25 or with LC16m8. The percentage of macrophages (CD11b^{+}F4/80^{+}) among IHLs and IL-6 production from these macrophages were significantly lower in rVV-N25-treated mice than in control mice (Figure 6G). Though the percentage of TNF-α-producing macrophages was not significantly different in rVV-N25-treated and control mice ($P = 0.099$), rVV-N25 treatment appeared to suppress these macrophages. These results demonstrated that rVV-N25 had a suppressive effect on activated macrophages, and they indicated that this suppression ameliorated the histological indicators of chronic hepatitis.

Discussion

Various HCV transgenic mouse models have been developed and used to examine immune response to HCV expression and the effects of pathogenic HCV protein on hepatocytes [4,16,17]. However, these transgenic mice develop tolerance to the HCV protein; therefore, examining immune response to HCV protein has been difficult.

To overcome the problem of immune tolerance in mouse models of HCV expression, we developed an HCV model in mice that relies on conditional expression of the core, E1, E2, and NS2 proteins and the Cre/loxP switching system [5,6]; we showed that the injection of an Ad-Cre vector enhanced the frequency of HCV-specific activated CD8 T cells in the liver of these mice and caused liver injury. However, the Ad-Cre adenovirus vector alone causes acute hepatitis in wild-type mice. Nevertheless, the transgenic model was useful for evaluating interactions between the host immune system and viral protein (serum ALT level over 2,000 IU/L) [5]; HCV core protein levels were reduced and expression of this protein was transient (about 2 weeks). Therefore, this Ad-Cre-dependent model cannot be used to effectively investigate immune responses to chronic HCV hepatitis.

Here, we used poly (I:C)-induced expression of Cre recombinase to generate HCV transgenic mice in order to study the effect of HCV protein and confirmed that these mice developed chronic active hepatitis–including steatosis, lipid deposition, and hepatocellular carcinoma. These pathological findings in the transgenic mice were very similar to those in humans with chronic hepatitis C; therefore, this mouse model of HCV may be useful for analyzing the immune response to chronic hepatitis. However, experimental results obtained with this mouse model may not directly translate to clinical findings from patients with HCV infection because the expression of HCV proteins was not liver specific in these mice. Furthermore, poly(I:C) injection can activate innate immune responses and, consequently, might induce temporary liver injury [18]. Additionally, poly(I:C) injection has an adjuvant effect; specifically, it stimulates TLR3 signaling [19].

To evaluate whether poly(I:C) injection caused hepatitis in CN2-29$^{(+/-)}$/MxCre$^{(-/-)}$ mice, we examined serum ALT levels and liver histology following poly(I:C) injection. We found that, following poly(I:C) injection, serum ALT levels in CN2-29$^{(+/-)}$/MxCre$^{(-/-)}$ mice increased, reached a peak one day after injection, declined from day 1 to day 6, and were not elevated thereafter; this time-course indicated that poly(I:C) injection alone did not induced continuous liver injury (figure S6). Based on these findings, we believe that the effects of poly(I:C) injection in these mice did not confound our analysis of chronic hepatitis.

Immunization with rVV-N25 suppressed HCV protein levels in the liver, and this suppression was associated with ameliorated pathological chronic hepatitis findings (see Figure 3). Importantly, rVV-N25 treatment did not cause liver injury based on the serum ALT levels; therefore, this treatment was unlikely to have cytopathic effects on infected hepatocytes. These findings provided strong evidence that rVV-N25 treatment effectively halted the progression of chronic hepatitis. Immunization with plasmid DNA or with recombinant vaccinia virus can effectively induce cellular and humoral immune responses and exert a protective effect against challenge with HCV infection [20,21]. However, findings from these previous studies revealed HCV immunization of both uninfected, naïve animals and immune-tolerant animals induced a HCV-specific immune response. In the model describe here; the animals were immune competent for HCV; therefore, our findings provided further important evidence that rVV-N25 was effective in the treatment of chronic hepatitis.

In addition, we demonstrated that rVV-N25 treatment in the absence of CD4 and CD8 T cells had no effect on HCV clearance. This important observation indicated that rVV-N25-induced HCV clearance was mediated by CD4 and CD8 T cells. Many studies have shown that spontaneous viral clearance during acute HCV infection is characterized by a vigorous, broadly reactive CD4 and CD8 T-cell response. [8,22] HCV clearance and hepatocellular cytotoxicity are both mediated by CD8 antigen-specific (cytotoxic T lymphocyte) CTLs [23]. Consistent with these observations, rVV-N25 treatment effectively induced the accumulation of NS2-specific CD8 T cells, which express high levels of

CD107a and IFN-γin the spleen. Notably, even with rVV-N25 immunization, the frequency of activated CD8 T cells was very low, and a minimum of 2-weeks incubation was required to distinguish the difference between rVV treatments. Even if a small population of specific CD8+ T cells played a relevant role in the reduction of core protein, it is difficult to assert that the only NS2-specific CD8+ T cells were important to this reduction. However, based on the results presented in Figure 4B, we are able to conclude that at least CD8+ and/or CD4+ T cells were important to the reduction in HCV core protein. Therefore, to elucidate the mechanism of HCV protein clearance, further investigation of not only the other T cell epitopes but also other immunocompetent cells is required.

Interestingly, rVV-N25 treatment–but not the rVV-CN2 or rVV-CN5 treatment–efficiently induced a HCV-specific activated CD8 T cells response; this difference in efficacy could have one or more possible causes. The HCV structural proteins (core, E1, and E2 proteins) in the rVV-CN construct may cause the difference; Saito et al. reported that injection with plasmid constructs encoding the core protein induced a specific CTL response in BALB/c mice [24]. Reportedly, CTL activity against core or envelope protein is completely absent from transgenic mice immunized with a plasmid encoding the HCV structural proteins, but core-specific CTL activity is present in transgenic mice that were immunized with a plasmid encoding the HCV core [21]. In contrast, when recombinant vaccinia virus expressing different regions of the HCV polyprotein were injected into BALB/c mice, only the HCV core protein markedly suppressed vaccinia-specific CTL responses [25]. Thus, the HCV core protein may have an immunomodulatory function [26]. Based on these reports and our results, we hypothesize that the causes underlying the effectiveness of rVV-N25 treatment were as follows: 1) this rVV construct included the core and envelope proteins and 2) the core protein had an immune-suppressive effect on CTL induction. Therefore, we suggest that exclusion of the core and envelope antigen as immunogen is one important factor in HCV vaccine design.

Interestingly, immunization with rVV-N25 rapidly suppressed the inflammatory response; however, immunization with either of the other rVVs did not (see Figure 6A). This result indicated that rVV-N25 may modulate inflammation via innate immunity, as well as via acquired immunity. Reportedly, Toll-like receptor (TLR)-dependent recognition pathways play a role in the recognition of poxviruses [27]. TLR2 and TLR9 have also been implicated in the recognition of the vaccinia virus [28,29]. These findings indicate that TLR on dendritic cells may modulate the immunosuppressive effect of rVV-N25 in our model of HCV infection; however, further examination of this hypothesis is required. The finding that pathological symptoms in the HCV transgenic mice were completely blocked by intravenous injection of TNF-α and IL-6 neutralizing antibodies indicated that the progression of chronic hepatitis depended on inflammatory cytokines in serum, rather than the HCV protein levels in hepatocytes. Lymphocytes, macrophages, hepatocytes, and adipocytes each produce TNF-α and IL-6 [30,31], and HCV-infected patients have elevated levels of TNF-α and IL-6 [32,33]. Both cytokines also contribute to the maintenance of hepatosteatosis in mice fed a high-fat diet [34], and production of TNF-α and IL-6 is elevated in obese mice due to the low grade inflammatory response that is caused by lipid accumulation [35]. These findings indicate that both cytokines are responsible for HCV-triggered hepatosteatosis, and anti-cytokine neutralization is a potential treatment for chronic hepatitis if antiviral therapy is not successful.

The reduction of macrophages in number might be due to the induction of apoptosis by vaccinia virus *in vitro* infection as previous reported [36]. To understand the mechanisms responsible for the reduction of the number of macrophage, we performed another experiment to confirm whether the macrophages were infected with vaccinia virus inoculation. However, based on PCR analyses; vaccinia virus DNA was not present in liver tissue that contained macrophages (Figure S7). Furthermore, apoptosis of macrophages was not detected in liver samples (Data not shown). Based on these results, it is unlikely that the reduction in the number of macrophages was due to apoptosis induced by vaccinia virus infection. Although rVV-N25 reduced the number of macrophage, precise mechanism is still unknown. Further examination to elucidate the mechanism is required.

In conclusion, our findings demonstrated that rVV-N25 is a promising candidate for an HCV vaccine therapy. Additionally, the findings of this study indicate that rVV-N25 immunization can be used for prevention of HCV infection and as an antiviral therapy against ongoing HCV infection.

Materials and Methods

Ethics Statement

All animal care and experimental procedures were performed according to the guidelines established by the Tokyo Metropolitan Institute of Medical Science Subcommittee on Laboratory Animal Care; these guidelines conform to the Fundamental Guidelines for Proper Conduct of Animal Experiment and Related Activities in Academic Research Institutions under the jurisdiction of the Ministry of Education, Culture, Sports, Science and Technology, Japan, 2006. All protocols were approved by the Committee on the Ethics of Animal Experiments of the Tokyo Metropolitan Institute of Medical Science (Permit Number: 11–078). All efforts were made to minimize the suffering of the animals.

Animals

R6CN2 HCV cDNA (nt 294–3435) [37] and full genomic HCV cDNA (nt 1–9611) [38,39] were cloned from a blood sample taken from a patient (#R6) with chronic active hepatitis (Text S1). The infectious titer of this blood sample has been previously reported [40]. R6CN2HCV and R6CN5HCV transgenic mice were bred with Mx1-Cre transgenic mice (purchased from Jackson Laboratory) to produce R6CN2HCV-MxCre and R6CN5HCV-MxCre transgenic mice, which were designated CN2-29$^{(+/-)}$/MxCre$^{(+/-)}$ and RzCN5-15$^{(+/-)}$/MxCre$^{(+/-)}$ mice, respectively. Cre expression in the livers of these mice was induced by intraperitoneal injection of polyinosinic acid–polycytidylic acid [poly(I:C)] (GE Healthcare UK Ltd., Buckinghamshire, England); 300 μL of a poly(I:C) solution (1 mg/mL in phosphate-buffered saline [PBS]) was injected three times at 48-h intervals. All animal care and experimental procedures were performed according to the guidelines established by the Tokyo Metropolitan Institute of Medical Science Subcommittee on Laboratory Animal Care.

Histology and Immunohistochemical Staining

Tissue samples were fixed in 4% paraformaldehyde in PBS, embedded in paraffin, sectioned (4-μm thickness), and stained with hematoxylin and eosin (H&E). Staining with periodic acid–Schiff stain, Azan stain, silver, or Oil-red-O was also performed to visualize glycogen degeneration, fibrillization, reticular fiber degeneration, or lipid degeneration, respectively.

For immunohistochemical staining, unfixed frozen liver sections were fixed in 4% paraformaldehyde for 10 min and then incubated with blocking buffer (1% bovine serum albumin in PBS) for 30 min at room temperature. Subsequently, the sections were incubated with biotinylated mouse anti-HCV core mono-

clonal antibody (5E3) for 2 h at room temperature. After being washed with PBS, the sections were incubated with streptavidin–Alexa Fluor 488 (Invitrogen). The nuclei were stained with 4',6-diamidino-2-phenylindole (DAPI). Fluorescence was observed using a confocal laser microscope (Laser scanning microscope 510, Carl Zeiss).

Generation of rVVs

The pBR322-based plasmid vector pBMSF7C contained the ATI/p7.5 hybrid promoter within the hemagglutinin gene region of the vaccinia virus, which was reconstructed from the pSFJ1-10 plasmid and pBM vector [41,42]. Separate full-length cDNAs encoding either the HCV structural protein, nonstructural protein, or all HCV proteins were cloned from HCV R6 strain (genotype 1b) RNA by RT-PCR. Each cDNA was inserted into a separate pBMSF7C vector downstream of the pBMSF7C ATI/p7.5 hybrid promoter; the final designation of each recombinant plasmid was pBMSF7C-CN2, pBMSF7C-N25, or pBMSF-CN5 (Figure 2). They were then transfected into primary rabbit kidney cells infected with LC16m8 (multiplicity of infection = 10). The virus–cell mixture was harvested 24 h after the initial transfection by scrapping; the mixture was then frozen at −80°C until use. The hemagglutinin-negative recombinant viruses were cloned as previously described [42] and named rVV-CN2, rVV-N25, or rVV-CN5. Insertion of the HCV protein genes into the LC16m8 genome was confirmed by direct PCR, and expression of each protein from the recombinant viruses was confirmed by western blot analysis. The titers of rVV-CN2, rVV-N25, and rVV-CN5 were determined using a standard plaque assay and RK13 cells.

Statistical Analysis

Data are shown as mean ± SD. Data were analyzed using the nonparametric Mann–Whitney or Kruskal–Wallis tests or ANOVA as appropriate; GraphPad Prism 5 for Macintosh (GraphPad) was used for all analyses. P values <0.05 were considered statistically significant.

Supporting Information

Figure S1 HAI score of liver samples taken from CN2-29$^{(+/-)}$/MxCre$^{(+/-)}$ mice.
(EPS)

Figure S2 Lipid degeneration in samples of liver taken from CN2-29$^{(+/-)}$/MxCre$^{(+/-)}$ mice.
(EPS)

Figure S3 HCV protein expression after infection of LC16m8, rVV-CN2, rVV-N25, or rVV-CN5 into HepG2 cells.
(EPS)

Figure S4 Effects of treatment with rVV-N25 in RzCN5-15$^{(+/-)}$/MxCre$^{(+/-)}$ mice.
(EPS)

Figure S5 Daily cytokine profiles of the serum from CN2-29$^{(+/-)}$/MxCre$^{(+/-)}$ mice during the week following inoculation with LC16m8, rVV-CN2, rVV-N25, or rVV-CN5.
(EPS)

Figure S6 The immune response following poly(I:C) injection in the acute phase.
(EPS)

Figure S7 Detection of vaccinia virus DNA in the skin, liver, and spleen after inoculation with attenuated vaccinia virus (Lister strain) or highly attenuated vaccinia virus (LC16m8 strain).
(EPS)

Table S1 Incidence of hepatocellular carcinoma in male and female transgenic mice at 360, 480, and 600 days after poly(I:C) injection.
(EPS)

Text S1 Supporting information including material and methods, and references.
(DOCX)

Acknowledgments

We thank Dr. Fukashi Murai for supporting this study. We also thank Dr. Keiji Tanaka for providing the MxCre mice, Dr. Shigeo Koyasu for providing the GK1.5 (anti-CD4) and 53–6.72 (anti-CD8) monoclonal antibodies, and Dr Takashi Tokuhisa for helpful discussions.

Author Contributions

Performed the experiments: SS KK TC Y. Tobita TO FY Y. Tokunaga. Analyzed the data: SS KK TC MK. Contributed reagents/materials/analysis tools: KT-K TW TT MM K. Mizuno YH TH K. Matsushima. Wrote the paper: SS KK MK. Study concept and design: MK.

References

1. Lauer GM, Walker BD (2001) Hepatitis C virus infection. N Engl J Med 345: 41–52.
2. Alter MJ (1995) Epidemiology of hepatitis C in the West. Semin Liver Dis 15: 5–14.
3. Kawamura T, Furusaka A, Koziel MJ, Chung RT, Wang TC, et al. (1997) Transgenic expression of hepatitis C virus structural proteins in the mouse. Hepatology 25: 1014–1021.
4. Moriya K, Fujie H, Shintani Y, Yotsuyanagi H, Tsutsumi T, et al. (1998) The core protein of hepatitis C virus induces hepatocellular carcinoma in transgenic mice. Nat Med 4: 1065–1067.
5. Wakita T, Katsume A, Kato J, Taya C, Yonekawa H, et al. (2000) Possible role of cytotoxic T cells in acute liver injury in hepatitis C virus cDNA transgenic mice mediated by Cre/loxP system. J Med Virol 62: 308–317.
6. Wakita T, Taya C, Katsume A, Kato J, Yonekawa H, et al. (1998) Efficient conditional transgene expression in hepatitis C virus cDNA transgenic mice mediated by the Cre/loxP system. J Biol Chem 273: 9001–9006.
7. Folgori A, Capone S, Ruggeri L, Meola A, Sporeno E, et al. (2006) A T-cell HCV vaccine eliciting effective immunity against heterologous virus challenge in chimpanzees. Nat Med 12: 190–197.
8. Chisari FV, Ferrari C (1995) Hepatitis B virus immunopathology. Springer Semin Immunopathol 17: 261–281.
9. Machida K, Tsukiyama-Kohara K, Seike E, Tone S, Shibasaki F, et al. (2001) Inhibition of cytochrome c release in Fas-mediated signaling pathway in transgenic mice induced to express hepatitis C viral proteins. J Biol Chem 276: 12140–12146.
10. Kuhn R, Schwenk F, Aguet M, Rajewsky K (1995) Inducible gene targeting in mice. Science 269: 1427–1429.
11. Li K, Chen Z, Kato N, Gale M Jr, Lemon SM (2005) Distinct poly(I-C) and virus-activated signaling pathways leading to interferon-beta production in hepatocytes. J Biol Chem 280: 16739–16747.
12. Sugimoto M, Yamanouchi K (1994) Characteristics of an attenuated vaccinia virus strain, LC16m0, and its recombinant virus vaccines. Vaccine 12: 675–681.
13. Youn JW, Hu YW, Tricoche N, Pfahler W, Shata MT, et al. (2008) Evidence for protection against chronic hepatitis C virus infection in chimpanzees by immunization with replicating recombinant vaccinia virus. J Virol 82: 10896–10905.
14. Guidotti LG, Rochford R, Chung J, Shapiro M, Purcell R, et al. (1999) Viral clearance without destruction of infected cells during acute HBV infection. Science 284: 825–829.
15. Burkett MW, Shafer-Weaver KA, Strobl S, Baseler M, Malyguine A (2005) A novel flow cytometric assay for evaluating cell-mediated cytotoxicity. J Immunother 28: 396–402.

16. Pasquinelli C, Shoenberger JM, Chung J, Chang KM, Guidotti LG, et al. (1997) Hepatitis C virus core and E2 protein expression in transgenic mice. Hepatology 25: 719–727.
17. Lerat H, Honda M, Beard MR, Loesch K, Sun J, et al. (2002) Steatosis and liver cancer in transgenic mice expressing the structural and nonstructural proteins of hepatitis C virus. Gastroenterology 122: 352–365.
18. Lang KS, Georgiev P, Recher M, Navarini AA, Bergthaler A, et al. (2006) Immunoprivileged status of the liver is controlled by Toll-like receptor 3 signaling. The Journal of clinical investigation 116: 2456–2463.
19. Jasani B, Navabi H, Adams M (2009) Ampligen: a potential toll-like 3 receptor adjuvant for immunotherapy of cancer. Vaccine 27: 3401–3404.
20. Elmowalid GA, Qiao M, Jeong SH, Borg BB, Baumert TF, et al. (2007) Immunization with hepatitis C virus-like particles results in control of hepatitis C virus infection in chimpanzees. Proc Natl Acad Sci U S A 104: 8427–8432.
21. Satoi J, Murata K, Lechmann M, Manickan E, Zhang Z, et al. (2001) Genetic immunization of wild-type and hepatitis C virus transgenic mice reveals a hierarchy of cellular immune response and tolerance induction against hepatitis C virus structural proteins. J Virol 75: 12121–12127.
22. Crispe IN (2009) The liver as a lymphoid organ. Annu Rev Immunol 27: 147–163.
23. Chisari FV (2005) Unscrambling hepatitis C virus-host interactions. Nature 436: 930–932.
24. Saito T, Sherman GJ, Kurokohchi K, Guo ZP, Donets M, et al. (1997) Plasmid DNA-based immunization for hepatitis C virus structural proteins: immune responses in mice. Gastroenterology 112: 1321–1330.
25. Large MK, Kittlesen DJ, Hahn YS (1999) Suppression of host immune response by the core protein of hepatitis C virus: possible implications for hepatitis C virus persistence. Journal of immunology 162: 931–938.
26. Dustin LB, Rice CM (2007) Flying under the radar: the immunobiology of hepatitis C. Annu Rev Immunol 25: 71–99.
27. Bowie A, Kiss-Toth E, Symons JA, Smith GL, Dower SK, et al. (2000) A46R and A52R from vaccinia virus are antagonists of host IL-1 and toll-like receptor signaling. Proc Natl Acad Sci U S A 97: 10162–10167.
28. Zhu J, Martinez J, Huang X, Yang Y (2007) Innate immunity against vaccinia virus is mediated by TLR2 and requires TLR-independent production of IFN-beta. Blood 109: 619–625.
29. Samuelsson C, Hausmann J, Lauterbach H, Schmidt M, Akira S, et al. (2008) Survival of lethal poxvirus infection in mice depends on TLR9, and therapeutic vaccination provides protection. J Clin Invest 118: 1776–1784.
30. Sheikh MY, Choi J, Qadri I, Friedman JE, Sanyal AJ (2008) Hepatitis C virus infection: molecular pathways to metabolic syndrome. Hepatology 47: 2127–2133.
31. Tilg H, Moschen AR, Kaser A, Pines A, Dotan I (2008) Gut, inflammation and osteoporosis: basic and clinical concepts. Gut 57: 684–694.
32. Malaguarnera M, Di Fazio I, Laurino A, Ferlito L, Romano M, et al. (1997) Serum interleukin 6 concentrations in chronic hepatitis C patients before and after interferon-alpha treatment. Int J Clin Pharmacol Ther 35: 385–388.
33. Larrea E, Garcia N, Qian C, Civeira MP, Prieto J (1996) Tumor necrosis factor alpha gene expression and the response to interferon in chronic hepatitis C. Hepatology 23: 210–217.
34. Park EJ, Lee JH, Yu GY, He G, Ali SR, et al. (2010) Dietary and genetic obesity promote liver inflammation and tumorigenesis by enhancing IL-6 and TNF expression. Cell 140: 197–208.
35. Gregor MF, Hotamisligil GS (2011) Inflammatory mechanisms in obesity. Annu Rev Immunol 29: 415–445.
36. Humlova Z, Vokurka M, Esteban M, Melkova Z (2002) Vaccinia virus induces apoptosis of infected macrophages. The Journal of general virology 83: 2821–2832.
37. Choo QL, Kuo G, Weiner AJ, Overby LR, Bradley DW, et al. (1989) Isolation of a cDNA clone derived from a blood-borne non-A, non-B viral hepatitis genome. Science 244: 359–362.
38. Tsukiyama-Kohara K, Tone S, Maruyama I, Inoue K, Katsume A, et al. (2004) Activation of the CKI-CDK-Rb-E2F pathway in full genome hepatitis C virus-expressing cells. J Biol Chem 279: 14531–14541.
39. Nishimura T, Kohara M, Izumi K, Kasama Y, Hirata Y, et al. (2009) Hepatitis C virus impairs p53 via persistent overexpression of 3beta-hydroxysterol Delta24-reductase. J Biol Chem 284: 36442–36452.
40. Shimizu YK, Purcell RH, Yoshikura H (1993) Correlation between the infectivity of hepatitis C virus in vivo and its infectivity in vitro. Proc Natl Acad Sci U S A 90: 6037–6041.
41. Yasui F, Kai C, Kitabatake M, Inoue S, Yoneda M, et al. (2008) Prior immunization with severe acute respiratory syndrome (SARS)-associated coronavirus (SARS-CoV) nucleocapsid protein causes severe pneumonia in mice infected with SARS-CoV. J Immunol 181: 6337–6348.
42. Kitabatake M, Inoue S, Yasui F, Yokochi S, Arai M, et al. (2007) SARS-CoV spike protein-expressing recombinant vaccinia virus efficiently induces neutralizing antibodies in rabbits pre-immunized with vaccinia virus. Vaccine 25: 630–637.

Virus Research 163 (2012) 405–409

Contents lists available at SciVerse ScienceDirect

Virus Research

journal homepage: www.elsevier.com/locate/virusres

Short communication

Translocase of outer mitochondrial membrane 70 induces interferon response and is impaired by hepatitis C virus NS3

Yuri Kasama[a], Makoto Saito[a], Takashi Takano[b], Tomohiro Nishimura[c], Masaaki Satoh[a,d], Zhongzhi Wang[a], Salem Nagla Elwy Salem Ali[a,e], Shinji Harada[e], Michinori Kohara[f], Kyoko Tsukiyama-Kohara[a,*]

[a] Department of Experimental Phylaxiology, Faculty of Life Sciences, Kumamoto University, 1-1-1 Honjo Kumamoto City, Kumamoto 860-8556, Japan
[b] Division of Veterinary Public Health, Nippon Veterinary and Life Science University, 1-7-1 Kyonan, Musashino, Tokyo 180-8602, Japan
[c] KAKETSUKEN, Kyokushi, Kikuchi, Kumamoto 869-1298, Japan
[d] Department of Virology I, National Institute of Infectious Diseases, Tokyo 162-8640, Japan
[e] Department of Medical Virology, Faculty of Life Sciences, Kumamoto University, Japan
[f] Department of Microbiology and Cell Biology, Tokyo Metropolitan Institute of Medical Science, 2-1-6 Kamikitazawa, Setagaya-ku, Tokyo 156-8506, Japan

ARTICLE INFO

Article history:
Received 5 September 2011
Received in revised form 13 October 2011
Accepted 13 October 2011
Available online 20 October 2011

Keywords:
HCV
Tom70
MAVS
IFN
IRF-3
NS3

ABSTRACT

Hepatitis C virus (HCV) elevated expression of the translocase of outer mitochondrial membrane 70 (Tom70). Interestingly, overexpression of Tom70 induces interferon (IFN) synthesis in hepatocytes, and it was impaired by HCV. Here, we addressed the mechanism of this impairment. The HCV NS3/4A protein induced Tom70 expression. The HCV NS3 protein interacted in cells, and cleaved the adapter protein mitochondrial anti-viral signaling (MAVS). Ectopic overexpression of Tom70 could not inhibit this cleavage. As a result, IRF-3 phosphorylation was impaired and IFN-β induction was suppressed. These results indicate that MAVS works upstream of Tom70 and the cleavage of MAVS by HCV NS3 protease suppresses signaling of IFN induction.

Type I interferon (IFN) induction is the front line of host defense against viral infection. Intracellular double-stranded RNA is a viral replication intermediate and contains pathogen-associated molecular patterns (PAMPS) (Saito et al., 2008) that are recognized by pathogen-recognition receptors (PRRs) to induce IFN. One PRR family includes the Toll-like receptors (TLRs), which are predominantly expressed in the endosome (Heil et al., 2004). Another route of IFN induction takes place in the cytosol through activation of specific RNA helicases, such as retinoic acid-inducible (RIG)-I and melanoma differentiation associated gene 5 (MDA5). The ligand for RIG-I is an uncapped 5′ triphosphate RNA, which is found in viral RNAs of the *Flaviviridae* family, including hepatitis C virus (HCV), paramyxovirus, and rhabdoviruses (Kato et al., 2006). MDA5 recognizes viruses with protected 5′ RNA ends, for example, picornaviruses (Hornung et al., 2006). The adapter protein that links the RNA helicase to the downstream MAPK, NF-κB, and IRF-3 signaling pathways is referred to as the mitochondrial anti-viral signaling (MAVS) protein (Seth et al., 2005); alternative names include IPS-1, interferon-promoter stimulator 1; VISA, virus-induced signaling adaptor; and CARDIF, CARD adapter inducing IFN. HCV nonstructural protein 3 (NS3) possesses a serine protease domain at the N terminus (amino acids (aa) 1–180) and has been found to cleave adaptor proteins, MAVS at aa 508 (Meylan et al., 2005) and Toll/IL-1R domain-containing adapter inducing IFN-β-deficient (TRIF at aa 372; Ferreon et al., 2005). These cleavages provoke abrogation of the induction of the IFN pathway.

The translocase of the outer membrane (TOM) is responsible for initial recognition of mitochondrial preproteins in the cytosol (Baker et al., 2007; Neupert and Herrmann, 2007). The TOM machinery consists of 2 import receptors, Tom20 and Tom70, and, along with several other subunits, comprises the general import pore (Abe et al., 2000). Recently, Tom70 was found to interact with MAVS (Liu et al., 2010). Ectopic expression or silencing of Tom70, respectively, enhanced or impaired IRF3-mediated gene expression and IFN-β production. Sendai virus infection accelerated the

* Corresponding author. Present address: Transboundary Animal Diseases Center, Faculty of Agriculture, Kagoshima University, 1-21-24 Korimoto Kagoshima-shi, Kagoshima 890-0065, Japan. Tel.: +81 99 285 3589/96 373 5560; fax: +81 99 285 3589/96 373 5562.
E-mail address: kkohara@kumamoto-u.ac.jp (K. Tsukiyama-Kohara).

0168-1702/$ – see front matter © 2011 Elsevier B.V. All rights reserved.
doi:10.1016/j.virusres.2011.10.009

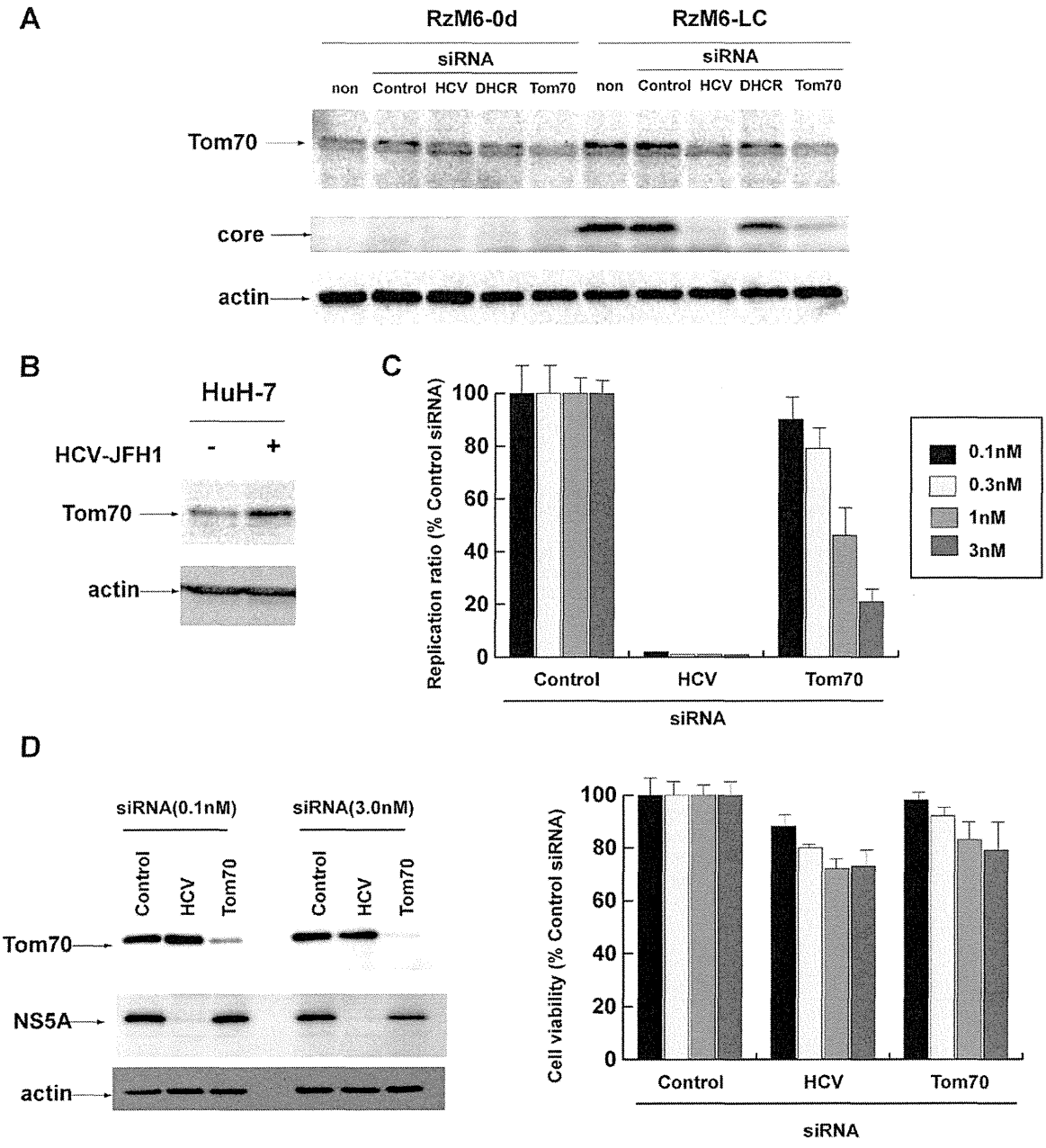

Fig. 1. HCV induces overexpression of Tom70 but impairs Tom70-induced IFN synthesis. (A) RzM6 cells (HCV-) and RzM6-LC cells (HCV+) were transfected with siRNAs of control (non-target siRNA#3: Thermo Fisher Scientific), HCV (R5: 5′-GUCUCGUAGACCGUGCAUCAuu-3′), DHCR24 (Nishimura et al., 2009), and Tom70 (Takano et al., 2011a). Control cells were mock-transfected. Tom70 protein was detected with MAb2-243a (Takano et al., 2011a) and actin protein was detected as an internal control (lower column). (B) HuH-7 cells were infected with HCV JFH-1 strain; Tom70 protein and actin protein were detected. (C) The HCV replicon cells (FLR3-1; Takano et al., 2011b) were transfected with siRNAs (control, HCV (R7: 5′-GUCUCGUAGACCGUGCACCAuu-3′), Tom70; 0.1, 0.3, 1, 3 nM) and HCV replication activity was measured with luciferase activity using the Bright-Glo luciferase assay kit (Promega). Cell viability was measured using WST-8 (Dojindo) reagent. Ratio with those of control siRNA treatment was calculated. Vertical bars were S.D. (D) HCV replicon cells (FLR3-1) were transfected with control, HCV (R7) and Tom70 siRNAs (0.1, 0.3 nM) and Tom70, NS5A and actin proteins were detected.

Tom70-mediated IFN induction and the interaction of Tom70 with MAVS. These recent findings indicated that Tom70 might be a critical mediator during IFN induction (Liu et al., 2010).

We previously observed that HCV induces Tom70 and is related to the apoptotic response (Takano et al., 2011a). However, no synergistic effect was observed for IFN induction by Tom70 and HCV. Therefore, in the present study, we have investigated the mechanism of modification of the Tom70-induced IFN synthesis pathway by HCV and clarified a finely balanced system regulated by viral protein.

The expression of Tom70 protein was examined using western blotting and modification by HCV was characterized (Fig. 1A). The level of Tom70 protein was increased in RzM6-LC cells compared with that in RzM6-0d cells (Tsukiyama-Kohara et al., 2004). The full-length HCV-RNA expression was induced by 4-hydroxytamoxifen (100 nM) and passaged for more than 44 days in RzM6-LC cells, and HCV expression was not induced in RzM6-0d cells. Silencing of HCV expression by siRNA (R5; Thermo Scientific) abolished core protein expression, and decreased the level of Tom70 protein expression in RzM6-LC cells (Fig. 1A). Silencing of Tom70 by siRNA significantly decreased the level of HCV core protein expression in RzM6-LC cells (Fig. 1A). The siRNA against 3-beta-hydroxysterol-delta24 reductase (DHCR24) slightly decreased the level of Tom70 protein. In contrast, the

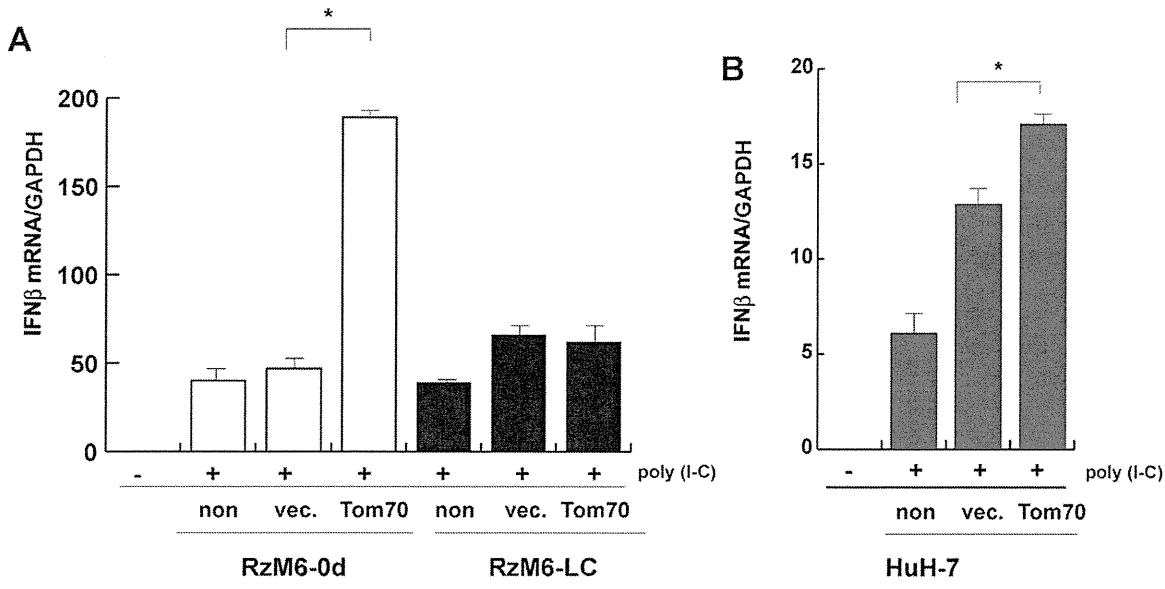

Fig. 2. Tom70-induced IFN synthesis was impaired by HCV. (A) RzM6-0d cells and LC cells were transfected with mock-vector, control pcDNA vector (vec.), or pcDNA-Tom70 expression vector, and the amount of IFN-β mRNA was measured by RTD-PCR and normalized to the amount of GAPDH mRNA using Gene expression assay kit (GE-Healthcare). Poly(I–C) (GE Healthcare) (5 μg) was transfected with RNAi Max reagent (Invitrogen) and IFN-βmRNA was measured after 6 h of poly(I–C) treatment. Vertical bars indicate S.D. $^*p < 0.05$. (B) HuH-7 cells were transfected with mock-vector, control vector, or Tom70 expression vector, and the amount of IFN-β mRNA was measured by RTD-PCR and normalized to the amount of GAPDH mRNA. Vertical bars indicate S.D. $^*p < 0.05$.

control siRNA did not have a significant effect on Tom70 protein expression.

We next examined the effects of HCV JFH-1 (Wakita et al., 2005) infection on Tom70 expression (Fig. 1B). Infection with HCV significantly increased the level of Tom70 protein expression. We also examine the role of Tom70 in HCV replication (Fig. 1C and D). Silencing of Tom70 by siRNA decreased the HCV replication in a dose dependent manner.

Thus, HCV induces Tom70 expression, and Tom70 is involved in viral replication.

It was recently shown that Tom70 recruits TBK1/IRF3 to mitochondria by binding to Hsp90 and inducing IFN-β synthesis (Liu et al., 2010). Therefore, we examined the effects of Tom70 overexpression on IFN synthesis and modification by HCV (Fig. 2). Level of IFN-β mRNA synthesis was quantitated by real-time detection (RTD) PCR. Overexpression of Tom70 by transfection of pcDNA6-Tom70 (Takano et al., 2011a) induced IFN-β mRNA synthesis in the absence of HCV after poly(I–C) treatment (RzM6-0d cells). However, the Tom70-mediated induction of IFN-β mRNA transcription was impaired in the presence of HCV (RzM6-LC cells) (Fig. 2A). Overexpression of Tom70 induced IFN-β mRNA synthesis in HuH-7 cells (Fig. 2B). Induction of IFN-β mRNA was lower in HuH-7 cells than HepG2 based RzM6 cells, which might be due to the defect in IFN induction system in HuH-7 cells (Preiss et al., 2008).

We have further addressed the mechanism of impairment of IFN-β mRNA transcription by HCV.

To identify the viral protein that was responsible for the induction of Tom70, we examined the Tom70 protein expression levels in HCV core, E1, E2, NS2, NS3/4A, NS4B, NS5A, and NS5B protein-expressing cells (data not shown), and Tom70 protein expression level was highest in the NS3/4A-expressing cells than was observed in cells expressing other proteins (Fig. 3A, data not shown), indicating an effect of HCV NS3/4A protein on Tom70 expression.

The expression vector of Myc- and His-tagged Tom70 was transfected into the empty control or NS3/4A-expressing cells and immunoprecipitated with anti-Myc antibody (Suppl. Fig. 1A). Results showed that Myc-Tom70 was precipitated in both cells (right panel) and NS3 protein was specifically precipitated by anti-Myc antibody in the NS3/4A-expressing cells (left panel). NS4A protein could not be detected (data not shown).

We next stained the NS3/4A-expressing cells with anti-NS3 and -Tom70 antibodies, and observed with confocal microscopy (Suppl. Fig. 1B). The signal of NS3 protein was clearly merged with that of Tom70, strongly supporting the possibility that the NS3 protein co-localizes with the Tom70 protein.

To clarify the effect of Tom70 on NS3, we transfected NS3/4A-expressing cells with the siRNA of Tom70 (Fig. 3A). Silencing of Tom70 decreased the level of NS3 protein in cells, but did not influence the levels of the MAVS and NF-κB proteins. These results suggest the possibility that Tom70 may increase the stability of NS3 protein in cells.

Tom70 reportedly interacts with MAVS during viral infection (Liu et al., 2010). Therefore, we examined the MAVS protein in cells expressing either the control empty or NS3/4A lenti-virus vector (Fig. 3B). Cleavage of MAVS (indicated as ΔMAVS) was observed in NS3/4A protein-expressing cells, as was reported previously (Meylan et al., 2005). Overexpression of Tom70 did not have a significant effect on the MAVS expression level and did not prevent MAVS cleavage by NS3. IRF-3 phosphorylation was suppressed in NS3/4A-expressing cells and was not influenced by Tom70 overexpression. The induction of IFN-β was impaired in NS3/4A-expressing cells, even in the presence of Tom70 overexpression (Fig. 3C). These data may indicate that MAVS exists upstream of Tom70 and that cleavage of MAVS by NS3/4A impaired the downstream signaling activation of IRF-3 phosphorylation (Suppl. Fig. 2).

Mitochondria provide a substantial platform for the regulation of IFN signaling. The MAVS adapter protein is a member of the family of RIG-I like receptors (RLRs), which links the mitochondria to the mammalian antiviral defense system (Seth et al., 2005). Proteomic studies have demonstrated that MAVS interacts with Tom70 (Liu et al., 2010). This interaction was accelerated by Sendai virus infection and synergized with ectopic expression of Tom70 to significantly increase the production of IFN-β (Liu et al., 2010). The results of the present study revealed that infection with HCV induced Tom70 expression, but the presence of HCV impaired IFN

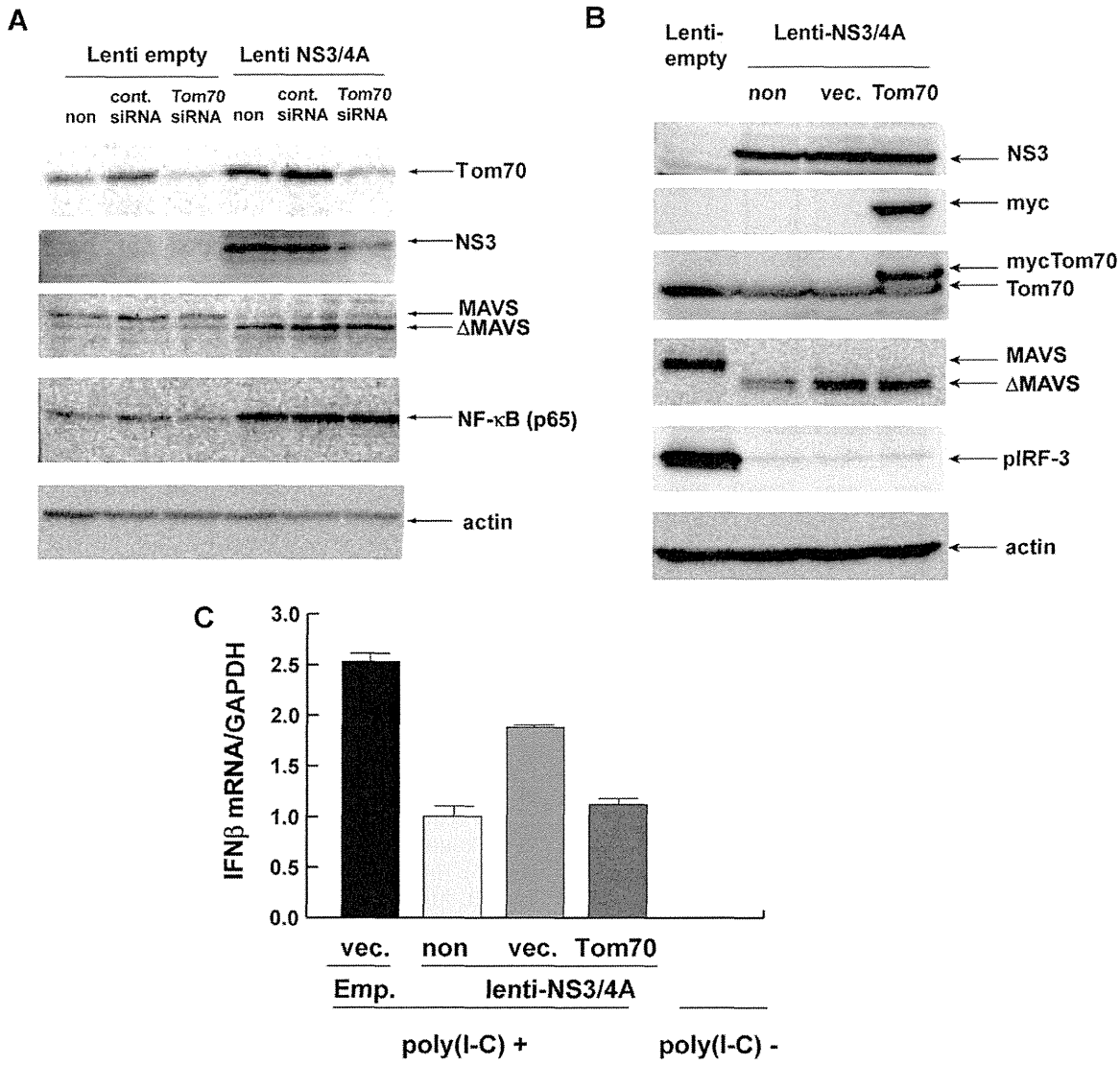

Fig. 3. Silencing of Tom70 decreased the level of NS3 and cleavage of MAVS by NS3/4A impaired IRF-3 phosphorylation even in the presence of Tom70. (A) Empty or NS3/4A-lenti virus vector expressing HepG2 cells were transfected with control siRNA and Tom70 siRNA or mock-transfected (non) as a control. MAVS, NS3, Tom70, and actin proteins were detected by western blot. (B) Empty or NS3/4A-expressing HepG2 cells were transfected with control pcDNA vector (vec.) and pcDNA6 (Invitrogen)-Tom70 or mock-transfected (non) as a control. NS3, Tom70, phosphorylated IRF-3, MAVS, and actin proteins were examined by western blot. (C) IFN-β mRNA was measured by RTD-PCR and normalized with GAPDH mRNA amount in empty or NS3/4A expressing cells with transfection of mock (non), pcDNA-vector (vec.) or pcDNA-Tom70 (Tom70). Poly(I–C) was treated, as described in the legend of Fig. 2.

induction. It has been reported that the C-terminal transmembrane domain (TM) of MAVS interacts with the N-terminal transmembrane domain of Tom70 (Liu et al., 2010). The HCV NS3 protein cleaves MAVS at residue 508 (Meylan et al., 2005), which should impair the interaction of MAVS and Tom70. This may attenuate the downstream signaling pathway (TBK-IRF3) and the induction of IFN synthesis (Suppl. Fig. 2). In our study, the level of NF-κB protein was not significantly influenced by Tom70 in the presence or absence of NS3. This may indicate that other pathways, such as TLR3 and downstream pathways, might compensate to maintain the NF-κB protein expression level in the absence of the MAVS-Tom70 signaling pathway.

Infection with HCV induced expression of Tom70, but the activation of the IFN signaling pathway was abrogated by the HCV NS3 protease. These findings indicate that recovery of the MAVS-Tom70 pathway may be a means to increase the efficacy of IFN therapy against HCV infection.

Recently, we observed that overexpression of Tom70 increased the resistance to the TNFα-induced apoptotic response (Takano et al., 2011a), indicating that Tom70 overexpression might contribute to the apoptotic resistance of HCV-infected cells and the establishment of persistent HCV infection. Thus, Tom70 might be a novel target for the regulation of HCV infection.

Acknowledgements

Authors thank Professor Yoshiharu Matsuura for providing the rabbit polyclonal NS5A antibody. This work was supported by grants from the Ministry of Health, Labor, and Welfare of Japan and the Ministry of Education, Culture, Sports, Science, and Technology of Japan.

Appendix A. Supplementary data

Supplementary data associated with this article can be found, in the online version, at doi:10.1016/j.virusres.2011.10.009.

References

Abe, Y., Shodai, T., Muto, T., Mihara, K., Torii, H., Nishikawa, S., Endo, T., Kohda, D., 2000. Structural basis of presequence recognition by the mitochondrial protein import receptor Tom20. Cell 100 (5), 551–560.

Baker, M.J., Frazier, A.E., Gulbis, J.M., Ryan, M.T., 2007. Mitochondrial protein-import machinery: correlating structure with function. Trends Cell Biol. 17 (9), 456–464.

Ferreon, J.C., Ferreon, A.C., Li, K., Lemon, S.M., 2005. Molecular determinants of TRIF proteolysis mediated by the hepatitis C virus NS3/4A protease. J. Biol. Chem. 280 (21), 20483–20492.

Heil, F., Hemmi, H., Hochrein, H., Ampenberger, F., Kirschning, C., Akira, S., Lipford, G., Wagner, H., Bauer, S., 2004. Species-specific recognition of single-stranded RNA via toll-like receptor 7 and 8. Science 303 (5663), 1526–1529.

Hornung, V., Ellegast, J., Kim, S., Brzozka, K., Jung, A., Kato, H., Poeck, H., Akira, S., Conzelmann, K.K., Schlee, M., Endres, S., Hartmann, G., 2006. 5′-Triphosphate RNA is the ligand for RIG-I. Science 314 (5801), 994–997.

Kato, H., Takeuchi, O., Sato, S., Yoneyama, M., Yamamoto, M., Matsui, K., Uematsu, S., Jung, A., Kawai, T., Ishii, K.J., Yamaguchi, O., Otsu, K., Tsujimura, T., Koh, C.S., Reis e Sousa, C., Matsuura, Y., Fujita, T., Akira, S., 2006. Differential roles of MDA5 and RIG-I helicases in the recognition of RNA viruses. Nature 441 (7089), 101–105.

Liu, X.Y., Wei, B., Shi, H.X., Shan, Y.F., Wang, C., 2010. Tom70 mediates activation of interferon regulatory factor 3 on mitochondria. Cell Res. 20 (9), 994–1011.

Meylan, E., Curran, J., Hofmann, K., Moradpour, D., Binder, M., Bartenschlager, R., Tschopp, J., 2005. Cardif is an adaptor protein in the RIG-I antiviral pathway and is targeted by hepatitis C virus. Nature 437 (7062), 1167–1172.

Neupert, W., Herrmann, J.M., 2007. Translocation of proteins into mitochondria. Annu. Rev. Biochem. 76, 723–749.

Nishimura, T., Kohara, M., Izumi, K., Kasama, Y., Hirata, Y., Huang, Y., Shuda, M., Mukaidani, C., Takano, T., Tokunaga, Y., Nuriya, H., Satoh, M., Saito, M., Kai, C., Tsukiyama-Kohara, K., 2009. Hepatitis C virus impairs p53 via persistent overexpression of 3beta-hydroxysterol Delta24-reductase. J. Biol. Chem. 284 (52), 36442–36452.

Preiss, S., Thompson, A., Chen, X., Rodgers, S., Markovska, V., Desmond, P., Visvanathan, K., Li, K., Locarnini, S., Revill, P., 2008. Characterization of the innate immune signalling pathways in hepatocyte cell lines. J. Viral Hepat. 15 (12), 888–900.

Saito, T., Owen, D.M., Jiang, F., Marcotrigiano, J., Gale Jr., M., 2008. Innate immunity induced by composition-dependent RIG-I recognition of hepatitis C virus RNA. Nature 454 (7203), 523–527.

Seth, R.B., Sun, L., Ea, C.K., Chen, Z.J., 2005. Identification and characterization of MAVS, a mitochondrial antiviral signaling protein that activates NF-kappaB and IRF 3. Cell 122 (5), 669–682.

Takano, T., Kohara, M., Kasama, Y., Nishimura, T., Saito, M., Kai, C., Tsukiyama-Kohara, K., 2011a. Translocase of outer mitochondrial membrane 70 expression is induced by hepatitis C virus and is related to the apoptotic response. J. Med. Virol. 83 (5), 801–809.

Takano, T., Tsukiyama-Kohara, K., Hayashi, M., Hirata, Y., Satoh, M., Tokunaga, Y., Tateno, C., Hayashi, Y., Hishima, T., Funata, N., Sudo, M., Kohara, M., 2011b. Augmentation of DHCR24 expression by hepatitis C virus infection facilitates viral replication in hepatocytes. J. Hepatol. 55 (3), 512–521.

Tsukiyama-Kohara, K., Tone, S., Maruyama, I., Inoue, K., Katsume, A., Nuriya, H., Ohmori, H., Ohkawa, J., Taira, K., Hoshikawa, Y., Shibasaki, F., Reth, M., Minatogawa, Y., Kohara, M., 2004. Activation of the CKI-CDK-Rb-E2F pathway in full genome hepatitis C virus-expressing cells. J. Biol. Chem. 279 (15), 14531–14541.

Wakita, T., Pietschmann, T., Kato, T., Date, T., Miyamoto, M., Zhao, Z., Murthy, K., Habermann, A., Krausslich, H.G., Mizokami, M., Bartenschlager, R., Liang, T.J., 2005. Production of infectious hepatitis C virus in tissue culture from a cloned viral genome. Nat. Med. 11 (7), 791–796.

Gene 496 (2012) 79–87

Contents lists available at SciVerse ScienceDirect

Gene

journal homepage: www.elsevier.com/locate/gene

Detergent-induced activation of the hepatitis C virus genotype 1b RNA polymerase

Leiyun Weng [a], Michinori Kohara [b], Takaji Wakita [c], Kunitada Shimotohno [d], Tetsuya Toyoda [a,b,e,*]

[a] Unit of Viral Genome Regulation, Institut Pasteur of Shanghai, Key Laboratory of Molecular Virology & Immunology, Chinese Academy of Sciences, 411 Hefei Road, Shanghai 200025, PR China
[b] Infectious Disease Regulation Project, Tokyo Metropolitan Institute of Medical Sciences, 1-6, Kamikitazawa 2-chome, Setagaya-ku, Tokyo 156-8506, Japan
[c] Department of Virology II, National Institute of Health, 1-23-1 Toyama, Shinjuku, Tokyo 132-8640, Japan
[d] Affiliated Research Institute, Chiba Institute of Technology, 2-17-1 Tsudamuna, Narashino, Chiba 275-0016, Japan
[e] Choju Medical Institute, Fukushimura Hospital, 19-4 Azanakayama, Noyori-cho, Toyohashi, Aichi 441-8124, Japan

ARTICLE INFO

Article history:
Accepted 18 January 2012
Available online 28 January 2012

Keywords:
HCV
NS5B
RNA polymerase
In vitro transcription
Triton X-100
Oligomer

ABSTRACT

Recently, we found that sphingomyelin bound and activated hepatitis C virus (HCV) 1b RNA polymerase (RdRp), thereby recruiting the HCV replication complex into lipid raft structures. Detergents are commonly used for resolving lipids and purifying proteins, including HCV RdRp. Here, we tested the effect of detergents on HCV RdRp activity in vitro and found that non-ionic (Triton X-100, NP-40, Tween 20, Tween 80, and Brij 35) and twitterionic (CHAPS) detergents activated HCV 1b RdRps by 8–16.6 folds, but did not affect 1a or 2a RdRps. The maximum effect of these detergents was observed at around their critical micelle concentrations. On the other hand, ionic detergents (SDS and DOC) completely inactivated polymerase activity at 0.01%. In the presence of Triton X-100, HCV 1b RdRp did not form oligomers, but recruited more template RNA and increased the speed of polymerization. Comparison of polymerase and RNA-binding activity between JFH1 RdRp and Triton X-100-activated 1b RdRp indicated that monomer RdRp showed high activity because JFH1 RdRp was a monomer in physiological conditions of transcription. Besides, 502H plays a key role on oligomerization of 1b RdRp, while 2a RdRps which have the amino acid S at position 502 are monomers. This oligomer formed by 502H was disrupted both by high salt and Triton X-100. On the contrary, HCV 1b RdRp completely lost fidelity in the presence of 0.02% Triton X-100, which suggests that caution should be exercised while using Triton X-100 in anti-HCV RdRp drug screening tests.

1. Introduction

Hepatitis C virus (HCV) belongs to the family *Flaviviridae* and has a positive-stranded RNA genome (Lemon et al., 2007). HCV chronically infects more than 130 million people worldwide (Wasley and Alter, 2000), and infection often induces liver cirrhosis and/or hepatocellular carcinoma (Kiyosawa et al., 1990; Saito et al., 1990). The 9.6-kb-long HCV RNA genome has a long open reading frame encoding a polyprotein of approximately 3,010 amino acids, which is processed into at least 10 viral proteins (NH_2-C-E1-E2-p7-NS2-NS3-NS4A-NS4B-NS5A-NS5B-COOH) by host and viral proteases (Grakoui et al., 1993; Hijikata et al., 1993). The 5′-untranslated region (UTR) contains the internal ribosome entry site (IRES) (Tsukiyama-Kohara et al., 1992). The 3′-UTR contains a poly pyrimidine "U/C" tract, a variable region, and 98-base X-region (Tanaka et al., 1996).

HCV RNA replication depends on the association between the viral protein and raft membranes (Shi et al., 2003; Aizaki et al., 2004), where NS5B RNA polymerase (RdRp) localizes by binding to sphingomyelin (Sakamoto et al., 2005). HCV RdRp is a key enzyme involved in the transcription and replication of the viral genome, and an important target of antivirals. Recently, we found that sphingomyelin bound to and activated HCV 1b RdRp, thereby recruiting the HCV replication complex into lipid raft structures (Weng et al., 2010).

Detergents are commonly used for solubilizing proteins from the lipid-containing components. Some restriction enzymes, reverse transcriptases, and Taq polymerases are stabilized by Triton X-100 or NP-40 (Weyant et al., 1990), while some other polymerases are activated by detergents (Thompson et al., 1972; Wu and Cetta, 1975; Hirschman et al., 1978). Triton X-100 is used for purification of HCV RdRp (Weng et al., 2009). Oligomerization of HCV RdRp is important for its activity (Qin et al., 2002; Clemente-Casares et al., 2011). We have developed an in vitro HCV de novo transcription system by using soluble RdRp and the complementary sequence of the 5′-HCV

Abbreviations: CHAPS, 3-[(3-cholanidopropyl)dimethylammonio]-1-propanesulfonate; CMC, critical micelle concentration; DOC, sodium deoxycholate; HCV, hepatitis C virus; IRES, internal ribosome entry site; KGlu, monopotassium glutamate; PMSF, phenylmethanesulfonyl fluoride; RdRp, RNA polymerase; SDS, sodium dodecyl sulfate; TNTase, terminal nucleotidyl transferase; UTR, untranslated region; nOG, octyl-β-glucoside.

* Corresponding author at: Choju Medical Institute, Fukushimura Hospital, 19-4 Azanakayama, Noyori-cho, Toyohashi, Aichi 441-8124, Japan. Tel.: +81 532 46 7511; fax: +81 532 46 8940.
E-mail address: toyoda_tetsuya@yahoo.co.jp (T. Toyoda).

0378-1119/$ – see front matter © 2012 Elsevier B.V. All rights reserved.
doi:10.1016/j.gene.2012.01.044

genome RNA (SL12-1S template) (Kashiwagi et al., 2002a; Kashiwagi et al., 2002b; Weng et al., 2009; Murayama et al., 2010; Weng et al., 2010). In this paper, we analyzed the effect of detergents on the activity and oligomerization of HCV RdRp, and found that non-ionic (Triton X-100, NP-40, Tween 20, Tween 80, and Brij 35) and twitterionic (3-[(3-cholanidopropyl)dimethylammonio]-1-propanesulfonate [CHAPS]) detergents activated HCV 1b RdRp. In addition, we analyzed the mechanism of RdRp activation by detergents and the relationship between RdRp oligomerization and its activity.

2. Materials and methods

2.1. Mutant HCV RdRp

The H502S mutation of HCR6 (1b) RdRp and the S502H mutation of JFH1 (2a) were introduced using an in vitro mutagenesis kit (Stratagene). Oligonucleotide sequence information is available upon request.

2.2. Purification of HCV RdRp from bacteria

HCV HCR6wt (1b) (Weng et al., 2009), NN (1b) (Watashi et al., 2005), Con1 (1b) (Binder et al., 2007), JFH1wt (2a) (Weng et al., 2009), J6CF (2a) (Murayama et al., 2007), H77 (1a) (Blight et al., 2003), RMT (1a), HCR6 (1b) H502S, and JFH1 (2a) H502S RdRps with a C-terminal 21-amino acid deletion were purified from bacteria as previously described with some modifications (Weng et al., 2009, 2010; Murayama et al., 2010). Briefly, HCV RdRps were eluted from Ni-NTA agarose (Qiagen) with 20 mM Tris–HCl (pH 8.0), 500 mM NaCl, 0.1% Triton X-100, 0.1% 2-mercaptoethanol, and 1 mM phenylmethanesulfonyl fluoride (PMSF) containing 250 mM imidazole after the column was washed with 5 mM imidazole. HCV RdRps were further purified through a Superdex 200 pg column (GE Healthcare) in 20 mM Tris–HCl (pH 8.0), 500 mM NaCl, 1 mM EDTA, 5 mM DTT, 10% glycerol, and 1 mM PMSF to remove contaminating nucleic acids (Fig. S1). The purified HCV RdRps were stored at −80 °C.

2.3. De novo HCV RdRp assay

HCV RdRp assay in the absence of primers was performed as described previously (Weng et al., 2009; Murayama et al., 2010). Briefly, following a 30-min pre-incubation period without ATP, CTP, or UTP, 100 nM HCV RdRp were incubated in 50 mM Tris–HCl (pH 8.0), 200 mM monopotassium glutamate (KGlu), 3.5 mM $MnCl_2$, 1 mM DTT, 0.5 mM GTP, 50 μM ATP, 50 μM CTP, 5 μM [α-^{32}P]UTP, 200 nM 184-nt model RNA template (SL12-1S) (Kashiwagi et al., 2002a; Weng et al., 2009; Murayama et al., 2010), 100 U/ml human placental RNase inhibitor, and the indicated amount of detergent at 29 °C for 90 min. [^{32}P]RNA products were separated in a 6% polyacrylamide gel containing 8 M urea. The resulting autoradiograph was analyzed with a Typhoon Trio Plus image analyzer (GE Healthcare) for the radio activity of 184-nt transcription products.

2.4. Kinetic analysis of HCV RdRp with and without Triton X-100

Kinetic analysis (measurement of *K*m and *V*max) was performed as previously published with and without 0.02% Triton X-100 (Kashiwagi et al., 2002b; Weng et al., 2009). For *K*m and *V*max of ATP, HCV RdRp was incubated in 50, 25, 10, 8, 5, 3, or 1 μM of ATP, 50 μM CTP, 0.5 mM GTP, 5 μM [α-^{32}P]UTP after preincubation in 0.5 mM GTP with and without 0.02% Triton X-100 at 29 °C for 60 min. For *K*m and *V*max of CTP, 50, 25, 10, 8, 5, 3, or 1 μM of CTP, 50 μM ATP, 0.5 mM GTP, and 5 μM [α-^{32}P]UTP, and for *K*m and *V*max of UTP, 50, 25, 10, 8, 5, 3, or 1 μM of UTP, 50 μM ATP, 0.5 mM GTP, 5 μM [α-^{32}P]CTP were used, respectively. For *K*m and *V*max of GTP, HCV RdRp was incubated in 500, 250, 100, 50, 25, 10, or 5 μM of GTP, 50 μM ATP, 50 μM CTP, 5 μM [α-^{32}P]UTP with and without 0.02% Triton X-100 without GTP preincubation.

2.5. Terminal nucleotidyl transferase (TNTase) assay

TNTase assay was performed with the heat denatured 5′-[^{32}P] sym/sub (5′-GAUCGGGCCCGAUC-3′) (Arnold and Cameron, 2000) with 0.5 mM GTP, 50 μM ATP, 50 μM CTP, and 50 μM UTP, and sym/sub with 0.5 mM GTP, 50 μM ATP, 50 μM CTP, and 5 μM [α-^{32}P]-UTP in the same experimental conditions as the above-described transcription assay (Hong et al., 2001). [^{32}P]RNA products were separated in a 15% polyacrylamide gel containing 8 M urea.

2.6. RNA filter-binding assay

RNA filter-binding assays were performed as previously described (Weng et al., 2009). Briefly, 100 nM of HCV RdRp and 100 nM [^{32}P] RNA template (SL12-1S) were incubated with the indicated amount of detergent in 25 μl of 50 mM Tris–HCl (pH 7.5), 200 mM KGlu, 3.5 mM $MnCl_2$, and 1 mM DTT at 29 °C for 30 min. After incubation, the solutions were diluted with 0.5 ml TE and filtered through nitrocellulose membranes (0.45 μm; Millipore). The filter was washed 5 times with TE, and the bound radioisotope was analyzed using the Typhoon Trio Plus image analyzer after being dried.

2.7. Western blot

Western blot analysis using a rabbit anti-HCV RdRp antibody was performed, as described previously (Kashiwagi et al., 2002b).

2.8. Gel filtration

The purified HCR6 (1b), J6CF (2a), and JFH1 (2a) RdRps (50 pmol) were applied on a Superdex 200 pg column in 50 mM Tris–HCl (pH 7.5), 200 mM KGlu or 150 mM NaCl, 3.5 mM $MnCl_2$, 1 mM DTT, and 0.2% glycerol with or without 0.1% Triton X-100.

2.9. Reagents

PMSF, Triton X-100, Tween 20, Tween 80, NP-40, Brij 35, octyl-β-glucoside (nOG), CHAPS, sodium deoxycholate (DOC), and sodium dodecyl sulfate (SDS) were obtained from Amresco; nucleotides were purchased from GE Healthcare; [α-^{32}P]UTP, [α-^{32}P]ATP, [α-^{32}P]GTP, [α-^{32}P]CTP, and [γ-^{32}P]ATP were from New England Nuclear.

2.10. Statistical analysis

Significant differences were determined using the Student's *t*-test.

3. Results

3.1. Effect of detergents on primer-independent HCV RdRp activity

First, we examined the effect of detergents on the primer-independent HCV RdRp activity in vitro (Fig. 1). HCR6 (1b) RdRpwt was activated by all the detergents tests, except octyl-β-glucoside (nOG), but JFH1 (2a) RdRpwt was not. The activation curves of HCR6 (1b) RdRpwt by these detergents plateaued at certain concentrations: 0.002 or 0.004% Triton X-100, 0.001% NP-40, 0.005% Tween 20, 0.001% Tween 80, 0.001% Brij 35, and 0.1% CHAPS. HCR6 (1b) RdRp activity decreased at concentrations greater than 1% Triton X-100, and 30% Triton X-100 completely inhibited HCR6 (1b) RdRpwt activity (Fig. 1A, right panel). With an activation ratio of about 2 at 0.1%, nOG weakly activated HCR6 (1b) RdRpwt. At 0.5% nOG, the

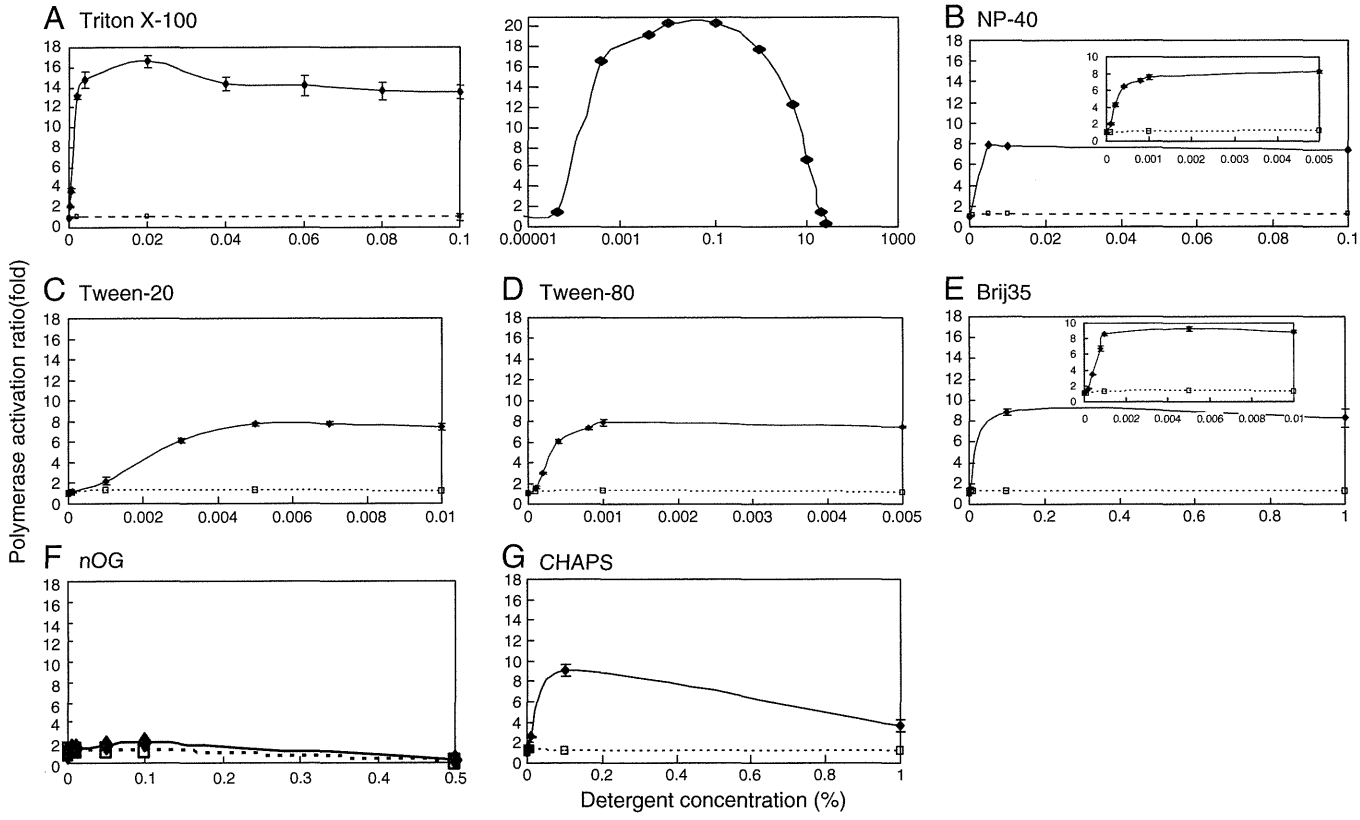

Fig. 1. The effect of detergents on HCV HCR6 and JFH1 RNA polymerases. Wild-type HCR6 (1b) and JFH1 (2a) RdRps were assayed with 0.000004, 0.00004, 0.0004, 0.004, 0.01, 0.02, 0.04, 0.06, 0.08, and 0.1% Triton X-100 (A, left panel); 0.0001, 0.0002, 0.0004, 0.0008, 0.001, 0.005, 0.1, and 0.5% NP-40 (B); 0.0001, 0.001, 0.003, 0.005, 0.007, and 0.01% Tween 20 (C); 0.0001, 0.0002, 0.0004, 0.0008, 0.001, and 0.005% Tween 80 (D); 0.0001, 0.0002, 0.0004, 0.0008, 0.001, 0.005, 0.01, 0.1, and 1% Brij 35 (E); 0.001, 0.005, 0.01, 0.05, and 0.1% nOG (F); or 0.0001, 0.001, 0.005, 0.01, 0.1, 0.1, and 1% CHAPS (G). The effect of high concentration of Triton X-100 on HCR6 (1b) RdRpwt is shown in A (right panel). Inset: Polymerase activation ratio at a lower concentration of NP-40 (B), and Brij 35 (E). Mean and standard deviation (error bar) of the polymerase activation ratio were calculated from 3 independent experiments. The solid line indicates the activation ratio of HCR6 (1b) RdRpwt, and the broken line indicates that of JFH1 (2a) RdRpwt.

activation ratio of HCR6 (1b) RdRpwt was 0.3. At 1% of CHAPS, the activity of HCR6 (1b) RdRpwt was increased by 3.6 folds. The detergent concentration that most activated HCR6 (1b) RdRpwt was approximate to the critical micelle concentration (CMC; Table 1).

When the activation ratios of detergents on HCR6 (1b) RdRpwt were compared, that of Triton X-100 was the highest (Fig. 2, Table 1). Other non-ionic detergents and CHAPS activated HCR6 (1b) RdRpwt to an extent equal to about half of Triton X-100 activation. Although a non-ionic detergent, nOG barely activated HCR6 (1b) RdRpwt.

Because 0.02% Triton X-100 maximally activated HCR6 (1b) RdRpwt, we compared its activation effect on other HCV RdRps (Fig. 3, Table 2). JFH1 (2a) RdRpwt showed the strongest RdRp activity, which is in accordance with previous reports (Weng et al., 2009; Murayama et al., 2010; Schmitt et al., 2011). The RdRp activities of 1b HCR6 and NN activated by Triton X-100 were similar to that of JFH1 RdRpwt in the absence of detergents (Fig. 3B), whereas the RdRp activity of Triton X-100-activated 1b Con1 was about half of that of wild-type JFH1. Neither 1a nor 2a RdRps were activated by Triton X-100.

Table 1
CMC and HCV HCR6 (1b) RdRpwt activation ratio of different detergents.

Detergent	CMC[a] in H_2O (%)	Minimal concentration of maximal activation (%)	Maximal activation (folds)[b]
Triton X-100	0.0155	0.02	16.6 ± 0.56
NP-40	0.0179	0.005	8.3 ± 0.18
Tween 20	0.0074	0.007	7.8 ± 0.21
Tween 80	0.0016	0.001	8.0 ± 0.22
Brij 35	0.1103	0.1	9.2 ± 0.34
nOG	0.672–0.730	0.1	2.1 ± 0.35
CHAPS	0.492–0.615	0.1	9.1 ± 0.60

[a] Modified from "TECHNICAL RESOURCE" (Pierce).
[b] Calculated from Fig. 2.

3.2. RNA template binding with Triton X-100

Next, we compared the template RNA-binding activity of 1a, 1b, and 2a RdRps in the presence of Triton X-100 by using the [^{32}P] SL12-1S model RNA template (Kashiwagi et al., 2002a; Weng et al., 2009, 2010; Murayama et al., 2010) in order to examine the transcription steps activated by Triton X-100 (Fig. 4, Table 2). Template RNA binding was the first step of transcription. The RNA-binding activity of JFH1 RdRpwt was the highest without Triton X-100 (data not shown) (Weng et al., 2009). Different from RdRp activity, the RNA-binding activity of all HCV RdRps was somehow activated by 0.02% Triton X-100. The RNA-binding activity of 1b RdRps was increased by 7–10 folds with Triton X-100.

3.3. Gel filtration of 1b and 2a RdRps

Proteins are generally soluble in detergents. Because HCR6 (1b) RdRpwt showed similar polymerase activity with Triton X-100 as JFH1 (2a) RdRpwt without Triton X-100, we compared the oligomerization state of these RdRps. The oligomerization state of HCR6 (1b) and JFH1 (2a) RdRps under transcription (physiological) conditions (200 mM KGlu or 150 mM NaCl) was analyzed by gel filtration on

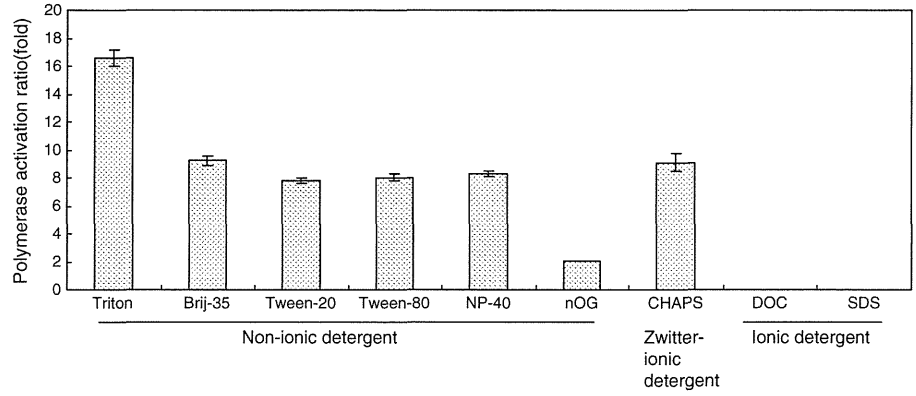

Fig. 2. Activation effect of HCV HCR6 polymerase with detergents at CMC. HCV HCR6 (1b) RdRpwt was assayed at CMC in the presence of Triton X-100 (0.02%), Brij 35 (0.1%), Tween 20 (0.007%), Tween 80 (0.001%), NP40 (0.005%), nOG (0.1%), CHAPS (0.1%), DOC (0.001%), and SDS (0.001%). The activation ratio (fold) is indicated in Table 2. Mean and standard deviation (error bar) of the polymerase activity relative to that without detergent were calculated from 3 independent experiments.

Superdex 200 (Figs. 5 and 6). HCR6 (1b) RdRpwt was eluted from the void volume fraction to the 158-kDa fraction without Triton X-100 (Fig. 5A), which meant that HCR6 (1b) RdRpwt formed random oligomers. It was eluted in the 38-kDa fraction with 0.1% Triton X-100 (Fig. 5B), which indicated that it was smaller than its monomer gel filtration size (Fig. S1D). However, JFH1 (2a) RdRpwt was eluted in the slightly larger fraction (80 kDa) than other HCV RdRps with or without Triton X-100, which indicated the monomer size (Figs. 5C and D, S1F). From the gel filtration and transcription data of HCR6 (1b) RdRpwt and JFH1 (2a) RdRpwt, it was concluded that Triton X-100 dispersed HCR6 (1b) RdRpwt, and that the higher-ordered oligomers of HCR6 (1b) RdRpwt were inactive. Triton X-100 might also affect the interaction between HCR6 (1b) RdRpwt and Superdex200 gel matrix because it was eluted in the smaller molecular weight fractions with Triton X-100 than the monomer gel-filtration size in 0.5 M NaCl (76 kDa, Fig. S1D). Western blot analysis indicated that these RdRp were not degraded (Figs. 5A and B, inset).

Qin et al. found that amino acids 18E and 502H interacted with each other to form the HCV 1b RdRp oligomer/dimer (Qin et al., 2002). Only 2a RdRps harbor the amino acid S at position 502, contrary to other genotype forms of RdRps, which harbor the amino acid H at that same position (Table S1). Therefore, we first examined

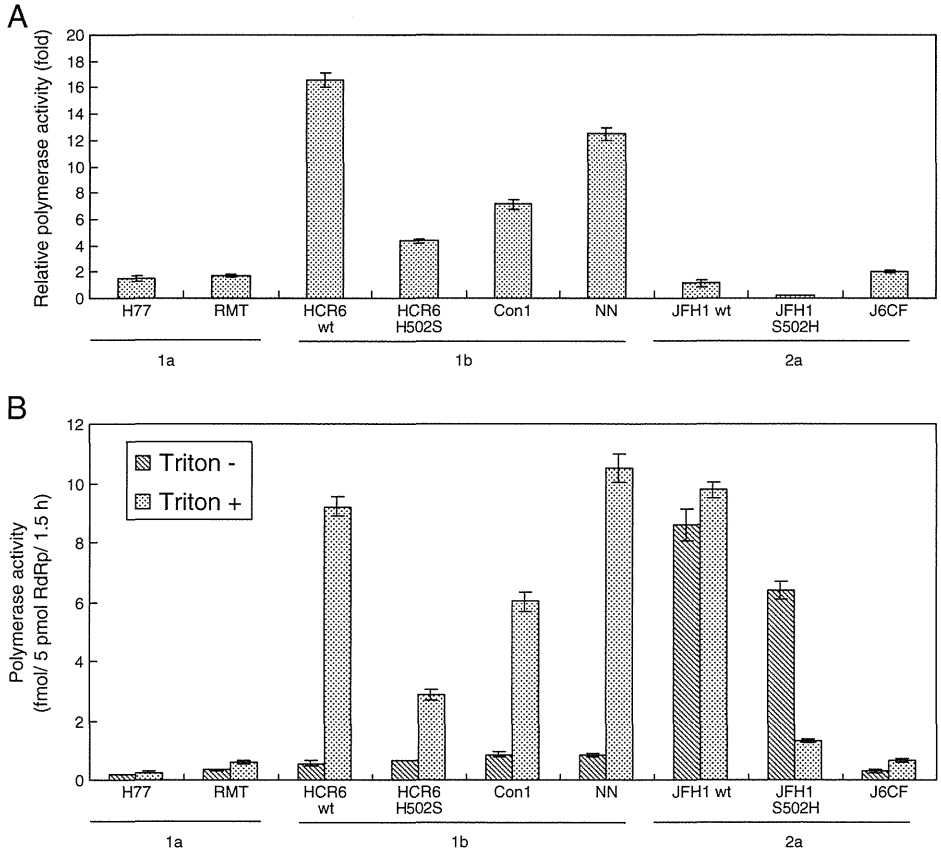

Fig. 3. Effect of 0.02% Triton X-100 on various HCV RNA polymerases. HCV H77 (1a), RMT (1a), HCR6 (1b) wt and H502S, NN (1b), Con1 (1b), JFH1 (2a) wt and S502H, and J6CF (2a) RdRps were assayed in the presence or absence of Triton X-100. A: Activation ratio (fold) of RNA polymerase activity. B: Polymerase activity (fmol of NMP/5 pmol RdRp/1.5 h) in the presence or absence of Triton X-100. Mean and standard deviation (error bar) of the polymerase activity were calculated from 3 independent experiments.

Table 2
Relative activation ratio of HCV RdRp by Triton X-100.

Genotype	1a		1b			2a	
Name	H77	RMT	HCR6	Con1	NN	JFH1	J6CF
Polymerase activity (folds)[a]	1.5 ± 0.17	1.7 ± 0.11	16.6 ± 0.56	7.1 ± 0.38	12.5 ± 0.48	1.1 ± 0.28	2.0 ± 0.12
RNA template-binding activity (folds)[b]	3.8 ± 0.11	3.9 ± 0.18	9.6 ± 0.39	7.9 ± 0.41	6.9 ± 0.16	2.2 ± 0.14	3.4 ± 0.21

[a] Activation ratio of polymerase activity was calculated on the basis of the data represented in Fig. 3A.
[b] Activation ratio of RNA template-binding activity was calculated on the basis of the data represented in Fig. 4A.

another 2a RdRp, J6CF (2a) RdRp, by gel filtration (Fig. 5E). J6CF (2a) RdRp was also eluted as a monomer in 150 mM NaCl buffer without Triton X-100. These gel filtration data was in agreement with the intermolecular interaction and random oligomerization of HCV RdRp caused by 18E and 502E (Qin et al., 2002). Amino acid 18E is shared by HCV RdRps of all 6 genotypes (Table S1) (Clemente-Casares et al., 2011). Therefore, in order to confirm the importance of 502H for oligomerization of HCV RdRp, S502H and H502S mutations were introduced into JFH1 (2a) and HCR6 (1b) RdRps, respectively, and analyzed by gel filtration (Fig. 6). JFH1 (2a) RdRpS502H formed oligomers, and HCR6 (1b) RdRpH502S was eluted in the 15-kDa fraction, which was smaller than its monomeric gel-filtration size. JFH1 (2a) RdRpS502H was eluted around the 50-kDa position with Triton X-100. The RdRp dimers (Qin et al., 2002) were not found in any of our gel filtration profiles. Western blot analysis indicated that the proteins were not degraded (Fig. 6, inset).

The effect of these mutations in RdRp and RNA template-binding activity with and without Triton X-100 was examined (Figs. 3 and 4). JFH1 (2a) RdRpS502H RdRp activity was lower than that of the wild-type in the absence of Triton X-100. Different from the Triton X-100 activation effect on HCR6 (1b) RdRpwt, JFH1 (2a) RdRpS502H RdRp activity decreased, while its RNA template binding increased, in the presence of Triton X-100. HCR6 (1b) RdRpH502S RdRp activity was similar to that of the wild-type, but less activated by Triton X-100 than by the wild-type. RNA template-binding activity of HCR6 (1b) RdRpH502S was activated 2.3 times by Triton X-100.

The 502 mutation data indicated that 502H is important for oligomerization of 1b RdRp molecules in the transcription (physiological salt) condition. Triton X-100 prevented the oligomerization of 1b RdRps by 502H. Moreover, For HCR6 (1b) RdRpwt, the 38-kDa gel filtration molecules (Fig. 5B), which might correspond to the monomer, were more active than the oligomer molecules.

3.4. Fidelity of HCV RdRp with Triton X-100

Finally, we aimed to calculate the kinetic constants (*K*m and *V*max) of HCR6 (1b) RdRp in the presence of 0.02% Triton X-100 because the activation ratio of the polymerase activity was higher than that of RNA binding of HCR6 (1b) RdRp. When nucleotide concentration was low, the amount of product without Triton X-100 decreased; this data can be used to draw Lineweaver–Burk plot (Weng et al., 2009). However, with Triton X-100, the product amount did not decrease according to the decrease of each nucleotide (Fig. 7A). Moreover, each of the nucleotide substrates was removed from the standard HCV in vitro transcription condition (Fig. 7B). Although ATP, CTP or UTP were removed from the reaction buffer, HCV HCR6 (1b) RdRp transcribed the same 184-nt products with Triton X-100, which disappeared without Triton X-100. When GTP was removed, no products were observed with or without Triton X-100 because HCV RdRp required GTP for its structure (Bressanelli et al., 2002). These kinetic experiments indicated that HCV HCR6 (1b) RdRp completely lost fidelity with Triton X-100.

Terminal nucleotidyl transferase (TNTase) activity has been sometimes detected in HCV 1b RdRp preparations (Behrens et al., 1996; Ranjith-Kumar et al., 2001; Ranjith-Kumar et al., 2004; Vo et al., 2004). TNTase activity was not detected in our system, in which the model RNA template contains a CCC-3′ at the 3′-end (Kashiwagi et al., 2002b; Weng et al., 2009). Nevertheless, we examined whether TNTase activity was detected with Triton X-100 using sym/sub, which has GpG-primed transcription activity, but we failed to observe any de novo initiation activity (Hong et al., 2001). No mobility shift was shown by 5′-[^{32}P]sym/sub or sym/sub incubated with [^{32}P]UTP on polyacrylamide gel electrophoresis (PAGE) (Figs. 7C and D), indicating that no TNTase activity was detected in our system with or without Triton X-100.

Apparent *K*m and *V*max of HCR6 (1b) RdRp with Triton X-100 for GTP was 303 ± 15.1 μM and 6.21 ± 0.225/min, respectively (Fig. S3).

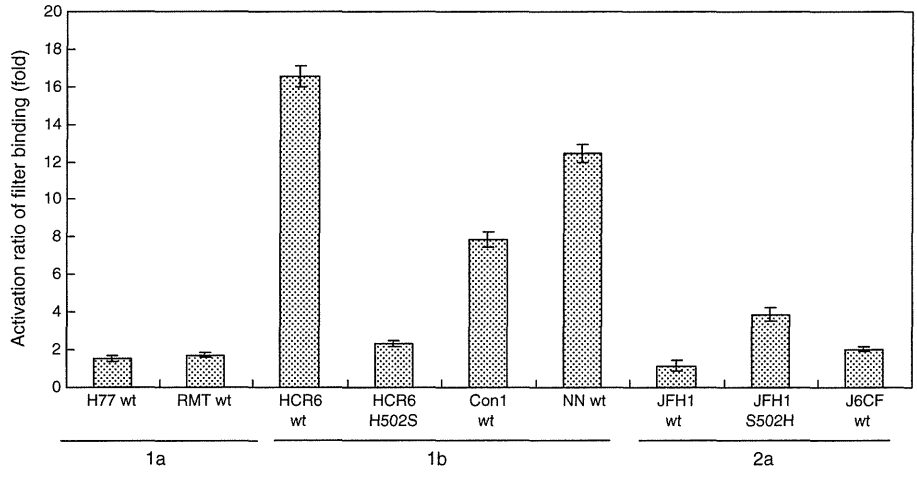

Fig. 4. Effect of 0.02% Triton X-100 on the RNA template-binding activity of HCV RNA polymerases. One hundred nanomolars each of HCV H77 (1a), RMT (1a), HCR6 (1b), NN (1b), Con1 (1b), JFH1 (2a), and J6CF (2a) RdRps with [^{32}P]RNA templates (SL12-1S) were filtered through nitrocellulose membranes after incubation with or without Triton X-100. Mean and standard deviation (error bar) of the RNA filter binding activation (folds) were calculated from 3 independent experiments.

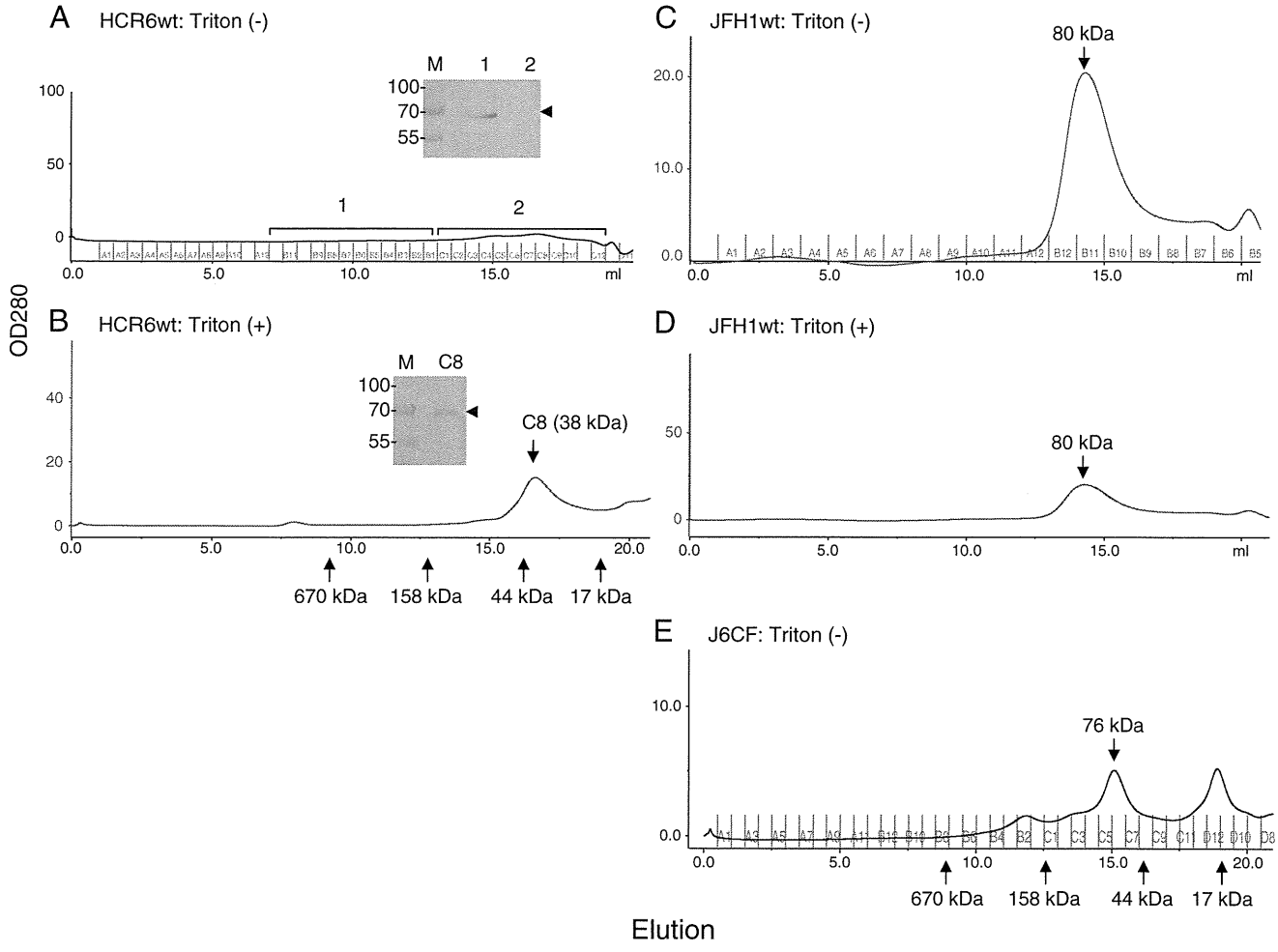

Fig. 5. Superdex 200 gel filtration of HCV HCR6 (1b), JFH1 (2a), and J6CF (2a) wild-type RNA polymerase with or without 0.1% Triton X-100. HCV HCR6 (1b) RdRpwt was applied on Superdex 200 gel filtration columns in 50 mM Tris–HCl (pH 7.5), 150 mM NaCl, 3.5 mM $MnCl_2$, 1 mM DTT, and 0.2% glycerol without (A) or with 0.1% Triton X-100 (B). HCV JFH1 (2a) RdRpwt was applied without (C) or with 0.1% Triton X-100 (D), and J6CF (2a) RdRp was applied without Triton X-100 (E) on the same columns. The elution position of the standard molecular weight markers is indicated below the graph. The molecular weight of the peak fraction is indicated in each graph. Inset in A: The fractions of the void volume—158 kDa (1) and those of lower molecular weight fractions (2) of HCR6 (1b) RdRpwt gel filtration without Triton X-100 were precipitated with TCA and analyzed by western blot. Inset in B: Fraction C8 of HCR6 (1b) RdRpwt with Triton X-100 was precipitated with TCA and analyzed by western blot. The position of HCR6 (1b) RdRpwt is indicated by an arrowhead. The position of the pre-stained size marker is indicated on the left side of the blots.

*K*m and *V*max of HCR6 (1b) RdRp without Triton X-100 for GTP was calculated as 54.7 ± 3.67 μM and 2.52 ± 0.108/min, respectively (Weng et al., 2009).

4. Discussion

Non-ionic (Triton X-100, NP-40, Tween 20, Tween 80, and Brij 35) and twitterionic (CHAPS) detergents activated HCV 1b RdRp by 7.2–16.6 folds when used at their CMC, but did not affect 1a or 2a RdRps (Figs. 1–3, Table 2). In turn, ionic detergents (SDS and DOC) completely inactivated polymerase activity at 0.01%. CMC is the minimum concentration at which a detergent forms micelles; above that concentration, a detergent exists as a large molecular weight complex. The CMC signifies the strength at which a detergent binds to proteins, i.e., low values indicate strong binding, whereas high values indicate weak binding. It is also an indication of the hydrophilicity of a detergent. Triton X-100, NP-40, and Brij 35 at CMC activated Moloney leukemia virus reverse transcriptase by interacting with the hydrophobic domain (Thompson et al., 1972). The activation mechanism of HCV RdRp by these detergents may be similar. However, the detergent interaction domain of HCV RdRp remains to be identified.

Triton X-100 is commonly used for purification of HCV RdRp from the bacteria and insect cells expressing this protein (Lohmann et al., 1997; Luo et al., 2000; Cramer et al., 2006; Weng et al., 2009). HCV 1b RdRp without the C-terminal hydrophobic region expressed in bacteria formed a large molecule complex in 0.1% Triton X-100 or 0.5% CHAPS with a low-salt buffer (<50 mM NaCl) (Qin et al., 2002; Wang et al., 2002). Under low-salt conditions, HCV RdRp was gel filtrated in void volume as a complex with contaminating nucleic acids, because HCV RdRp binds to RNA during purification without high-salt (0.5 M NaCl) stripping (Figs. S1 and S2). Therefore, the presence of HCV 1b RdRp in the void volume fraction of gel filtration by Wang et al. (Wang et al., 2002) could rather represent the complex of HCV RdRp with contaminating nucleic acids. Nevertheless, they also found monomers of HCV 1b RdRp in the gel filtration buffer containing 0.5% CHAPS, which activated polymerase activity (Fig. 1G). Detection of the monomeric HCV 1b RdRps by gel filtration in a buffer containing Triton X-100 and CHAPS has also been reported by other groups (Qin et al., 2002; Wang et al., 2002). HCR6 (1b) RdRpwt formed oligomers in physiological conditions without Triton X-100. In the presence of Triton X-100, HCR6 (1b) RdRpwt was eluted as the monomer which gel-filtration size was smaller than its size in 0.5 M NaCl (Fig. S1D) or calculated from its amino acid composition (64 kDa). HCV 2a (JFH1 and J6CF) RdRps formed a monomer in the same buffer without Triton X-100. Gel filtration analysis of 502 mutants of JFH1 (2a) and HCR6 (1b) RdRps have confirmed that 502H

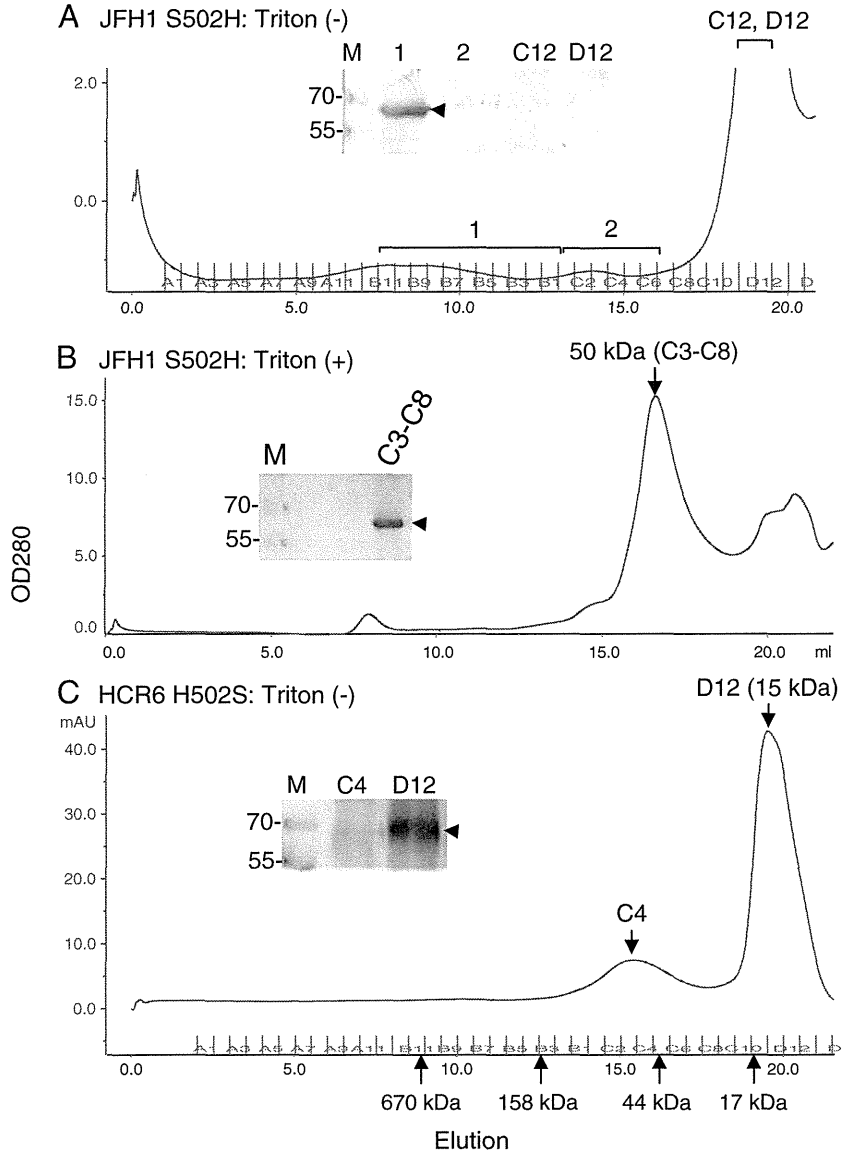

Fig. 6. Superdex 200 gel filtration of HCV JFH1 (2a) and HCR6 (1b) 502 mutant RNA polymerases. JFH1 (2a) S502H (A), and HCR6 (1b) H502S RdRps (C) were applied on Superdex 200 gel filtration columns in 50 mM Tris–HCl (pH 7.5), 150 mM NaCl, 3.5 mM $MnCl_2$, 1 mM DTT, and 0.2% glycerol. JFH1 (2a) RdRpS502H was also applied with 0.1% Triton X-100 (B). Inset in A: The fractions of the void volume—158 kDa (1), those of lower molecular weight fractions (2), fractions C12, and D12 of JFH1 (2a) RdRpS502H gel filtrations were precipitated with TCA and analyzed by western blot. Inset in B: Fraction C3–C8 of JFH1 (2a) RdRpS502H in Triton X-100 were precipitated with TCA and analyzed by western blot. Inset in C: Fractions C4 and D12 of HCR6 (1b) RdRpH502S were precipitated with TCA and analyzed by western blot. The position of HCV RdRp is indicated by an arrowhead. The position of the pre-stained size marker is indicated on the left side of the blots.

is important for the intermolecular interaction of HCV 1b RdRp (Qin et al., 2002). HCV RdRps without the C-terminal hydrophobic domain were soluble in high-salt buffer (>300 mM NaCl; Fig. S1) (Ferrari et al., 1999). The shift to the delayed elution of gel-filtration of HCR6 (1b) RdRpwt and JFH1 (2a) RdRp S502H with Triton X-100, and HCR6 (1b) RdRpH502S may come from the interaction of the RdRps with Superdex200 gel matrix induced by the mutations and Triton X-100.

Our data of HCV RdRp oligomerization at 502H (Fig. 6) are in agreement with those by Qin et al. (Qin et al., 2002), but are contradictory to those obtained by more sensitive methods (fluorescence resonance energy transfer [FRET] and yeast two-hybrid system) (Wang et al., 2002; Clemente-Casares et al., 2011). Interactions between a charged amino acid (His) and an aromatic residue (Trp) (Fernandez-Recio et al., 1997; Matthews et al., 1997; Takeuchi et al., 2003), or His–Glu interactions (Marti and Bosshard, 2003), are often found in proteins. JFH1 (2a) RdRpwt did not form dimers (Chinnaswamy et al., 2010). 502H may interact with 125 W in αF (Clemente-Casares et al., 2011), but not with 18E (Qin et al., 2002). This interaction is dissociated both with high-salt (Fig. S1) and with Triton X-100 (Figs. 5 and 6). Taken together, 502H of HCV 1b RdRp is important for oligomer formation in transcription (physiological salt) conditions. Besides the oligomerization using 502H, the αF and αT helixes of HCV RdRp, which were proposed to be involved in oligomerization (Clemente-Casares et al., 2011), may also be involved in oligomerization of the molecules in transcription condition. The 502 mutations in HCR6 (1b) and JFH1 (2a) RdRps are likely to affect the structure of the template channel by affecting the helix structures of the thumb domain (Bressanelli et al., 2002; Chinnaswamy et al., 2008) because the polymerase and RNA template binding activity of these mutant RdRps was not activated by Triton X-100 (Figs. 3 and 4). These findings indicate the importance around amino acid 502H for HCV 1b RdRp structure. However, these data contradict to the previous reports (Qin et al., 2002; Clemente-Casares et al., 2011).

Comparing the polymerase and template RNA-binding activity of JFH1 (2a) and HCR6 (1b) RdRps with and without Triton X-100,

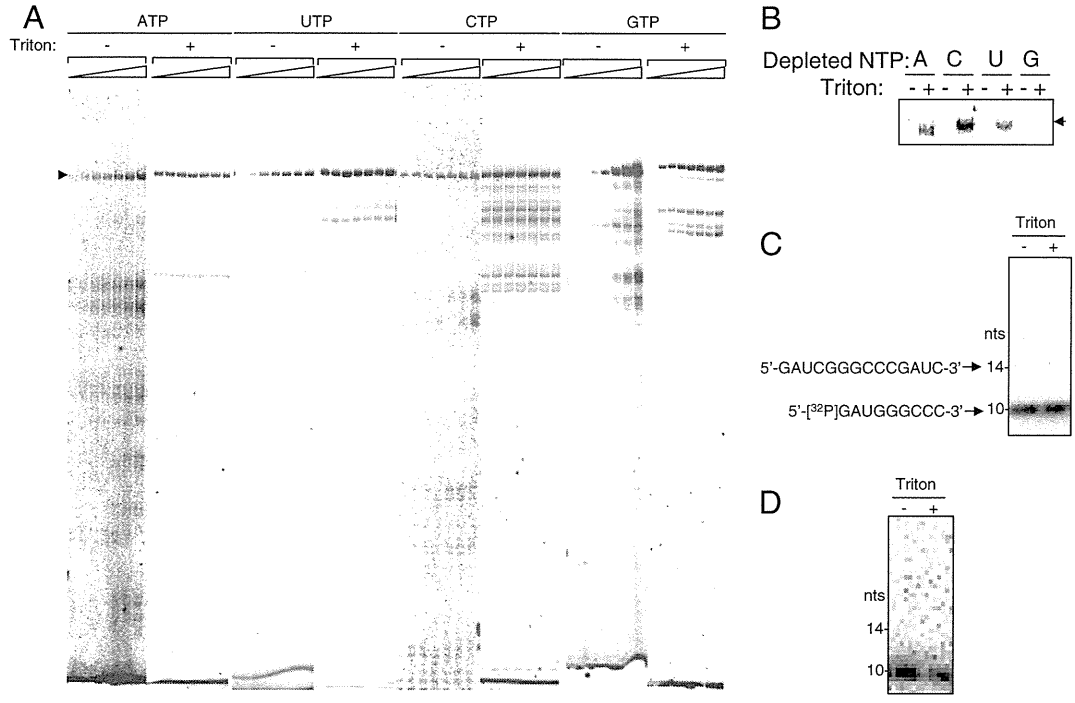

Fig. 7. Effect of substrate concentrations on in vitro transcription of HCR6 (1b) wild-type RNA polymerase, and TNTase activity in the presence of Triton X-100. A: Effect of nucleotide concentration on HCV HCR6 (1b) RdRpwt in vitro transcription with (+) and without (−) 0.02% Triton X-100. The concentration of ATP, UTP, and CTP varied from 1 to 50 μM, and that of GTP varied from 5 to 500 μM. B: Effect of nucleotide depletion on HCV HCR6 (1b) RdRpwt in vitro transcription with (+) and without (−) 0.02% Triton X-100. The position of 184-nt products is indicated by an arrowhead (A and B). C: TNTase activity of HCV HCR6 (1b) RdRpwt. 5′-[^{32}P]sym/sub was transcribed by HCV HCR6 (1b) RdRpwt with (+) and without (−) 0.02% Triton X-100. D: TNTase activity of HCV HCR6 (1b) RdRpwt. sym/sub was transcribed with [^{32}P]UTP by HCV HCR6 (1b) RdRpwt with (+) and without (−) 0.02% Triton X-100. The position of 10-nt sym/sub and 14-nt is indicated on the left.

RdRp which formed oligomer using 502H did not show high polymerase activity (Figs. 3–6). The inactive oligomer may be a part of the reason why a small fraction, less than 1%, of the purified HCV BK RdRp which belonged to 1b participated productively in transcription in vitro (Carroll et al., 2000). Taking together the data obtained by FRET (Clemente-Casares et al., 2011) and yeast two-hybrid systems (Wang et al., 2002), dynamic intermolecular interactions may occur under transcription conditions through the αT helix where amino acid 502 is located. The reason why only 1b RdRp was activated with Triton X-100 although RNA binding of all the RdRps tested was enhanced with Triton X-100, is not clear.

In case of JFH1 (2a) RdRp, the interaction with Triton X-100 may be different from that of HCR6 (1b) RdRp because it was not activated with Triton X-100 (Figs. 1 and 3), and because its gel-filtration profile was not affected with Triton X-100 (Fig. 5). This may be the reason of the inhibition of polymerase activity of JFH1 (2a) RdRpS502H by Triton X-100 although it was also disrupted to monomer (Figs. 3 and 6).

Triton X-100 activated only HCV 1b RdRp (Figs. 3 and 4). The closed conformation of HCV RdRp is required for de novo initiation (Chinnaswamy et al., 2008). With and without Triton X-100, JFH1 (2a) RdRpwt showed as high polymerase activity as HCR6 (1b) RdRpwt did with Triton X-100 (Fig. 3B). The very closed conformation of JFH1 (2a) RdRp is proposed to facilitate de novo initiation and high polymerase activity (Simister et al., 2009). Triton X-100 may also help the conformational change of HCR6 (1b) RdRp to the very closed conformation like that of JFH1 (2a) RdRp during transcription initiation.

HCV RdRp was co-purified with nucleic acids (Figs. S1 and S2). The contaminating nucleic acids were removed from HCV RdRp by high salt treatment. The contaminating nucleic acids carry proteins that have affinity to them, which misleads HCV in vitro transcription data. They also oligomerize HCV RdRp by crosslinking them. In a similar way, the contaminating nucleic acids in HCV RdRp preparations may mislead the binding data of HCV RdRp with other proteins.

From the activation kinetics of the detergents (Fig. 1, Table 1), the polymerase activation of 1b RdRp is likely to depend on the micelle formation of the detergent and on the direct interaction between RdRp and the detergents. The reason why the non-ionic detergent nOG did not activate the HCV RdRp is not known (Figs. 1 and 2).

The interaction mechanism of Triton X-100 and HCV 1b RdRp may be similar as that of sphingomyelin and HCV 1b RdRp because their activation kinetics were similar and the activated genotype was the same (Weng et al., 2010). Sphingomyelin activated only HCV 1b, but did not activate 1a or 2a RdRps. Both the activation curve of sphingomyelin and that of Triton X-100 showed the linear increase of polymerase activity. Then, sphingomyelin reached plateau at 20 molecules, and Triton X-100 reached plateau around its CMC.

Data about TNTase activity of HCV RdRp are controversial (Behrens et al., 1996; Ranjith-Kumar et al., 2001, 2004; Vo et al., 2004). In our system, TNTase activity was not detected with or without Triton X-100 (Figs. 7C and D).

GTP binds to HCV RdRp both as substrate and as a component of RdRp (Bressanelli et al., 2002). The apparent *K*m for GTP with Triton X-100 indicated that the substrate affinity dropped as low as to lose fidelity (Table 1, Figs. 7A and B). Triton X-100 may have affected the substrate-binding although its mechanism is not clear. HCV 1b full-length RdRp transcription activity obtained with CHAPS (Wang et al., 2002) might be that without fidelity as shown with Triton X-100. Detergents should not be used while screening substrate inhibitors of HCV RdRp. These data indicate that caution should be exercised while using detergents in anti-HCV RdRp drug screening tests.

Supplementary materials related to this article can be found online at doi:10.1016/j.gene.2012.01.044.

Acknowledgments

We thank Dr. J. Bukh, Dr. C. Rice, and Dr. R. Bartenshlager for providing pJ6CF, pHCVrepl3(S2204I)Neo, and Con1, respectively. This